https://doi.org/10.5194/cp-2021-89
Preprint. Discussion started: 16 July 2021

Climate of the Past Discussions
Open Access
EGU

Melt in the Greenland EastGRIP ice core reveals Holocene warming events

Julien Westhoff[1], Giulia Sinnl[1], Anders Svensson[1], Johannes Freitag[2], Helle Astrid Kjær[1], Paul Vallelonga[1], Bo Vinther[1], Sepp Kipfstuhl[2], Dorthe Dahl-Jensen[1,3], and Ilka Weikusat[2,4]

[1]Niels Bohr Institute, University of Copenhagen, Copenhagen, Denmark
[2]Alfred-Wegener-Institut Helmholtz-Zentrum für Polar- und Meeresforschung, Bremerhaven, Germany
[3]Centre for Earth Observation Science, University of Manitoba, Canada
[4]Department of Geosciences, Eberhard Karls University Tübingen, Germany

Correspondence: Julien Westhoff (julien.westhoff@nbi.ku.dk)

Abstract.

We present a record of melt events obtained from the EastGRIP ice core, in central north eastern Greenland, covering the largest part of the Holocene. The data were acquired visually using an optical dark-field line scanner. We detect and describe bubble free layers and -lenses throughout the ice above the bubble-clathrate transition, located at 1100 m in the EastGRIP ice core, corresponding to an age of 9720 years b2k. We distinguish between melt layers (bubble free layers continuous over the width of the core), melt lenses (discontinuous), crusts (thin and sharp bubble free layers) and attribute three levels of confidence to each of these, depending on how clearly they are identified. Our record of melt events shows a large, distinct peak around 1014 years b2k (986 CE) and a broad peak around 7000 years b2k corresponding to the Holocene Climatic Optimum. We analyze melt layer thicknesses and correct for ice thinning, we account for missing layers due to core breaks, and ignore layers thinner than 1.5 mm. We define the brittle zone in the EastGRIP ice core from 650 m to 950 m depth, where we count on average more than three core breaks per meter. In total we can identify approximately 831 mm of melt (corrected for thinning) over the past 10,000 years. We compare our melt layer record to the GISP2 and Renland melt layer records. Our climatic interpretation matches well with the Little Ice Age, the Medieval and Roman Warm Periods, the Holocene Climatic Optimum, and the 8.2 kyr event. We also compare the most recent 2500 years to a tree ring composite and find an overlap between melt events and tree ring anomalies indicating warm summers. We open the discussion for sloping bubble free layers (tilt angle off horizontal $> 10°$) being the effect of rheology and not climate. We also discuss our melt layers in connection to a coffee experiment (coffee as a colored substitute for melt infiltration into the snow pack) and the real time observations of the 2012 CE rain event at NEEM. We find that the melt event from 986 CE is most likely a large rain event, similar to 2012 CE, and that these two events are unprecedented throughout the Holocene. Furthermore, we suggest that the warm summer of 986 CE, with the exceptional melt event, was the trigger for the first Viking voyages to sail from Iceland to Greenland.

https://doi.org/10.5194/cp-2021-89
Preprint. Discussion started: 16 July 2021

Climate of the Past Discussions

1 Introduction

1.1 Greenland melt layer records

Melt layers provide a robust record of warm summer days on the Greenland ice sheet, meaning that the surface temperature exceeded the melting point and/or that insolation was very high (Langway and Shoji, 1990). The first full Holocene melt layer record from a Greenlandic ice core was presented by Alley and Anandakrishnan (1995) on the Greenland Ice Sheet Project 2 (GISP2) ice core, who applied visual inspection during ice core processing. Visual inspection was also used by Herron et al. (1981), some years earlier, on the DYE3 ice core from southern Greenland, to create a 2200 year melt record. Similar visual methods, in addition to density measurements, were used by Freitag et al. (2014 EGU poster) on two shallow cores around DYE3 and South Dome in Greenland. Shorter records have been established at other southern Greenland sites, such as site A (70,8 °N, 36,0 °W, 3145 m, Alley and Koci, 1988) or site J (66°51.9'N, 46°15.9'W, 2030 m, Kameda et al., 1995).

A range of techniques have been applied to investigate melt layers in ice cores from Greenland and other locations: Keegan et al. (2014) compared multiple shallow cores across the dry zone in Greenland and show a spatial variability of melt layers, with only the warm summer event from 1889 CE being visible in all cores (cores were drilled before 2012 CE). Studies of melt features in the ablation zone of the Greenland ice sheet have been conducted using multiple shallow ice cores (e.g. Graeter et al., 2018), or snow pits (e.g. Humphrey et al., 2012). Combined micro computer tomography (CT, Schaller et al., 2016) and visual analysis using line scan images (see methods section) for melt layer detection was applied on the Renland Ice Cap (RECAP) ice core, coastal eastern Greenland, by Taranczewski et al. (2019), combining one deep and two shallow cores. Melt layer records have been established for many glaciated sites around the world, e.g. in Canada (Koerner and Fisher, 1990; Fisher et al., 1995, 2012), Alaska (Winski et al., 2018), and Arctic Russia (Fritzsche et al., 2005).

There are several methods to detect melt layers in ice. They can be detected using noble gases (Orsi et al., 2015), irregularities in the Electronic Conductivity Measurements (ECM, pers. comm. Sune Rasmussen), or by identifying anomalies in stable water isotope records (Valerie Morris, in prep.). More recent melt events can be detected using satellite images: as an example Steen-Larsen et al., 2011 describe six recent melt events at the Northern Hemisphere Eemian Drilling Campaign (NEEM) site. Combining satellite and ice core data to create a melt archive is done in several studies such as (e.g. Mote, 2007; Keegan et al., 2014; Trusel et al., 2018). Melt layers, i.e. bubble free layers, can easily be confused with wind crusts (see method section), that are studied by Fegyveresi et al. (2018) and Weinhart et al. (2021).

The 2012 CE melt and rain event in Greenland, is very well observed and documented (e.g. Nghiem et al., 2012; Tedesco et al., 2013; Nilsson et al., 2015; Bonne et al., 2015). Bonne et al. (2015) provide a detailed study on the atmospheric conditions leading to the rain event, in combination with field observations (e.g. from Steen-Larsen et al., 2011). Nilsson et al. (2015) present a detailed study on the 2012 melt event using CryoSat-2 radar altimetry. Observations at the NEEM drill site show, that the surface temperature exceeded the melting point over five days, and that melt layers formed at approximately 5, 20, and 69 cm depth (Nghiem et al., 2012). Using the words of Trusel et al. (2018): "For the most recent 350 years in Greenland ice core, 2012 melt is unambiguously the strongest melt season on record."

https://doi.org/10.5194/cp-2021-89
Preprint. Discussion started: 16 July 2021

Climate of the Past Discussions
Open Access
EGU

55 ## 1.2 What are melt layers?

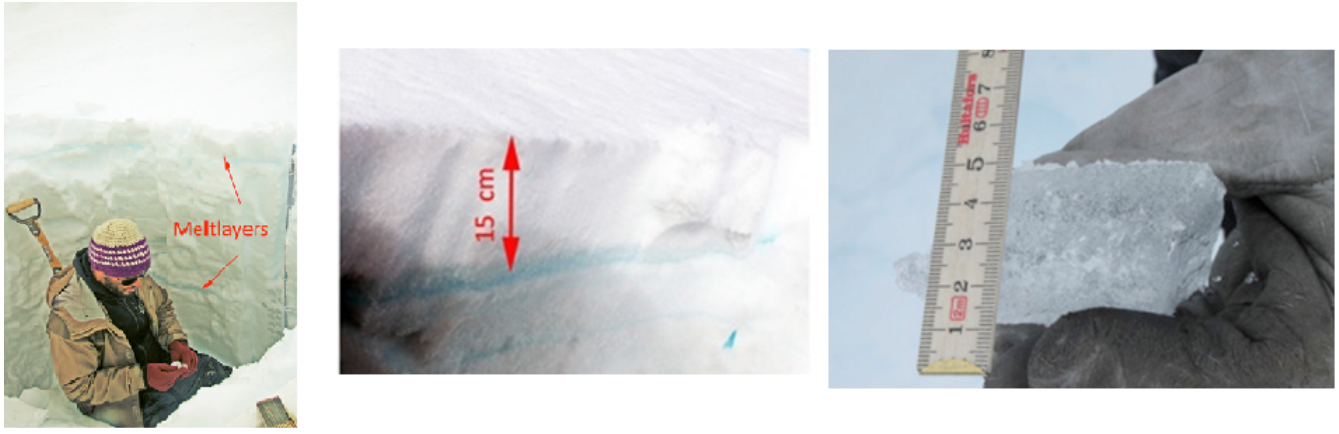

Figure 1. a) View into the snowpit dug just after the 2012-rain/melt event at NEEM. The resulting melt layers occur in depths of around 15 and 70 cm below surface. b) close up on the upper melt layer and c) the 3.5 centimeter thick layer.

Melt layers are commonly thought of as events with surface melt due to intense solar radiation and/or high temperature leading to the formation of superficial liquid melt puddles followed by their percolation into the snowpack (e.g. Shoji and Langway, 1987; Humphrey et al., 2012). Occurring less frequently, rain events over an ice sheet can lead to the same type of features, which was e.g. observed at NEEM in 2012 CE (fig. 1).

60 The exact influence of solar radiation on melt layers is still debated. As solar radiation is at the top of the atmosphere, the more correct term would be solar irradiance. However, Ohmura (2001) argue that it is not only solar irridiance, shortwave radiation, what is needed to initiate melting, but a positive radiation balance - in fact a positive energy balance is the precondition.

Ohmura (2001) states that the ice sheets exist because of high irradiance. This is used to sublimate snow if there are no clouds and no longwave radiation from the clouds. The clouds form the greenhouse and block the outgoing thermal radiation.
65 Sublimation needs eight times more energy than melting. So melting conditions are only reached if there is longwave radiation from the atmosphere and that means lots of clouds, since otherwise the reflected shortwave radiation is lost to space, and radiation and energy balance are negative. Eye witnesses from NEEM, DYE3, and South Dome in Greenland, verify, that thick clouds brought in the high air temperatures leading to the 2012 CE warm event across Greenland.

For recent melt events, it has been shown that these are spatially highly variable and only a widspread melt event from
70 1889 CE can be found in almost all shallow ice cores across Greenland (Keegan et al., 2014). Melt, or bubble free, layer records for the past 10,000 years have only been identified for the GISP2 (Alley and Anandakrishnan, 1995) and the RECAP (Taranczewski et al., 2019) ice cores. In deep ice cores, such as GISP2, bubbles transform to clathrates and become difficult to detect visually (Kipfstuhl et al., 2001). Methods to detect melt layers from clathrate distributions have not succeeded yet. In the RECAP ice core, the Holocene ice covers 533 of a total core length of 584 meters (Simonsen et al., 2019). Here the stratigraphy
75 of the deepest layers of the Holocene (early Holocene) are thinned too much to detect single melt layers. Therefore, all analysis

https://doi.org/10.5194/cp-2021-89
Preprint. Discussion started: 16 July 2021

Climate of the Past Discussions
Open Access
EGU

to date are limited to the past 10,000 years, with the exception of Orsi et al. (2015), who investigated noble gas (isotopes) on selected samples of the NEEM ice core.

The features in the snowpack resulting from a melt event can be distinguished into: melt layers, melt lenses (Das and Alley, 2005), and melt pipes (Pfeffer and Humphrey, 1998). Layers and lenses are horizontal structures with different lateral extensions and melt pipes are vertical pathways formed by the meltwater (more details in the methods section). In the next section, we present a simple experiment to reconstruct melt features in the snowpack.

1.3 The coffee experiment

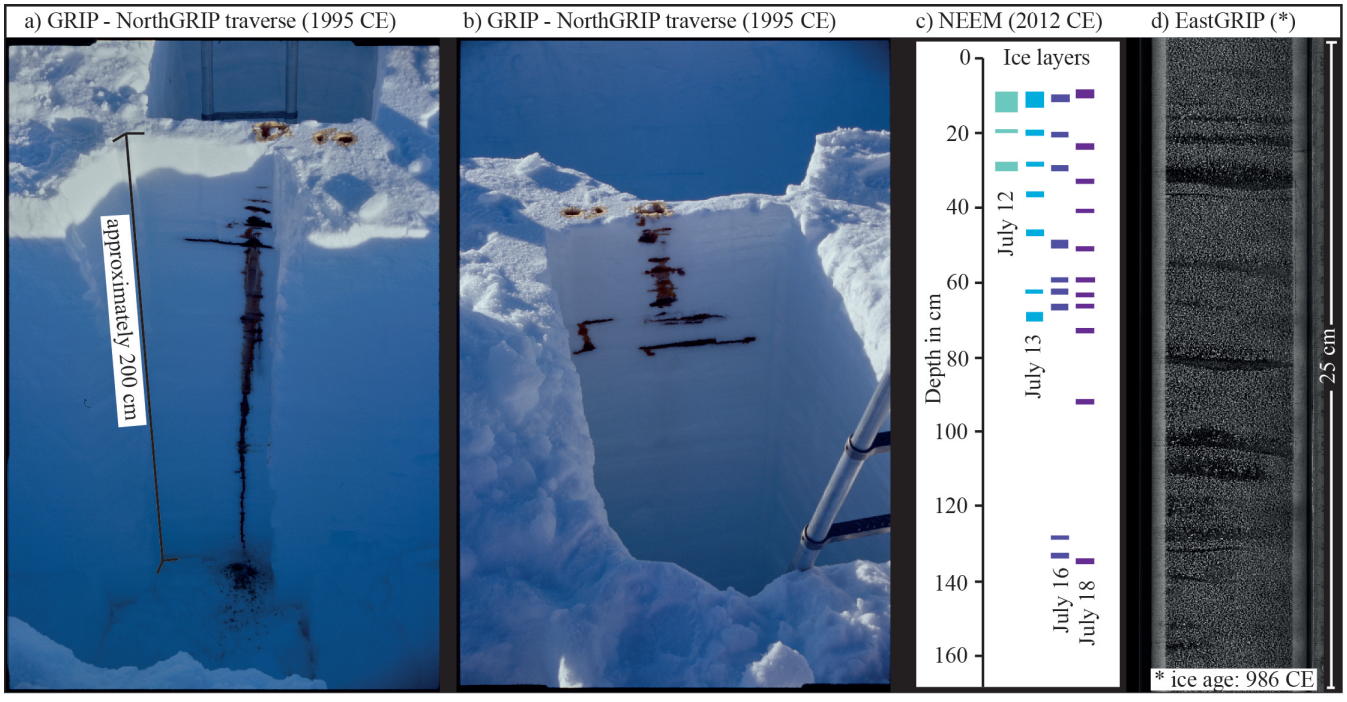

Figure 2. a,b) Two sides of the same double trench, with three coffee injection points visible on the surface of the trench wall. Vertical coffee-pipes are not always visible, but the horizontal coffee layers and lenses are very pronounced. The long vertical pipe reaching the bottom in a) is due to the ex-filtration of coffee from the trench wall. The trench's depth is approximately two meters. c) appearance of ice layers in different depths during the warm event 2012 at NEEM. Measurements are from the same snow pit, which was revisited over the days of the warm event. d) Upper half of line scan of bag 252 (top at 138.05 m depth, years 986 to 989 CE) with multiple melt lenses and layers.

We present the result from a simple rain-melt-event-experiment performed in April 1995, on a traverse from the Greenland Ice Core Project (GRIP) site to the Northern Greenland Ice Core Project (NorthGRIP) site in Greenland (fig. 2a,b). A double trench was dug, leaving an approximately 30 cm thick wall between the two trenches. This is commonly done to visualize different structures in the snowpack (e.g. Fegyveresi et al., 2018). Three shots of cold coffee were poured at the top of the

https://doi.org/10.5194/cp-2021-89
Preprint. Discussion started: 16 July 2021


Climate of the Past Discussions

trench wall simulating a melt event. The coffee percolates through the snowpack, leaving a brown trace representing melt layers, -lenses and -pipes. A more sophisticated version of this experiment was performed a decade later, between 2007 and 2009, by Humphrey et al. (2012) in western Greenland.

1.4 Real-time observations of the 2012 melt event

While ice core studies on melt events show the finished picture of melt layers, lenses, and pipes in the snowpack, the 2012 melt event at NEEM offered a unique chance to observe the creation of these structures in real-time. The warm event in 2012 lasted from July 12th to 15th, with varying temperatures around 0 °C (Bonne et al., 2015). During these days, snowpits reveal the appearance of ice layers at different depths over time (fig. 2c). Depth is relative to the snow surface and due to the warming of the snowpack, the whole surface level lowered about 10 to 15 cm over the course of the warm event. This explains the apparent "rise" of the uppermost ice level over time - the surface was actually lowering. The depth registration of each ice layer also slightly changes, due to a widening of the trench of approximately 0.5 m every measurement day. This shows the high spatial variability of ice- or melt layers in the snowpack.

By July 12, a substantial warming of the surface snowpack was observed, with the top 12 cm of snowpack close to melting point (-0.2 °C) and the development of more ice or refrozen melt layers at depths 22 and 32 cm. The surface snowpack had warmed considerably by July 13, with further thickening of melt layers and the development of a 3.5 cm-thick melt layer at 70 cm depth (fig. 1c). Local rain contributed to this rapid warming of the top 65 cm of snowpack to near-melting temperatures. Somewhat cooler conditions on July 14 saw some cooling of the lower part of the snowpack. July 15 was the last day of warming observed in the snowpack, with the uppermost 80 cm of snowpack near melting point, warming of deeper snow down to 1.5 m depth, and the deeper percolation of meltwater to 1.5 m depth. Observations of July 16 indicate a cooling of the snowpack from both above and below, with complete refreezing of the surface snow by July 18.

Experimental simulations of melt events have been performed by (Das and Alley, 2005; Humphrey et al., 2012), but in-situ observations have only been conducted at NEEM (e.g. Bonne et al., 2015) and Summit in 2012 (e.g. Bennartz et al., 2013). Older melt events can be found in ice cores using visual methods (fig. 2d), such as the line scanner (see methods section).

1.5 Climate of the Holocene

Melt layers, such as those resulting from the 2012 CE warm event, can be found in ice cores throughout the Holocene. To analyze and understand these, a climatic overview is necessary: Axford et al. (2021) have put together different records of the Holocene climate in Greenland (fig. 3), including the GISP2 melt layer record (Alley and Anandakrishnan, 1995). Their study offers two possible climatic reconstructions: A climatic optimum around the early Holocene, as shown by pollen, geological records, and $\delta 15N$ from ice cores (e.g. fig. 3c), or a damped climatic optimum, as shown by ice cores (fig. 3d). The dampening of these warm temperatures at the end of the Last Glacial Period and the early Holocene, is due to a larger ice sheet with higher surface elevation (fig. 3a, h), and therefore cooler temperatures, from ice core reconstructions, due to a higher lapse rate (e.g. Brunt, 1933; Gardner et al., 2009; Vinther et al., 2009).

https://doi.org/10.5194/cp-2021-89
Preprint. Discussion started: 16 July 2021

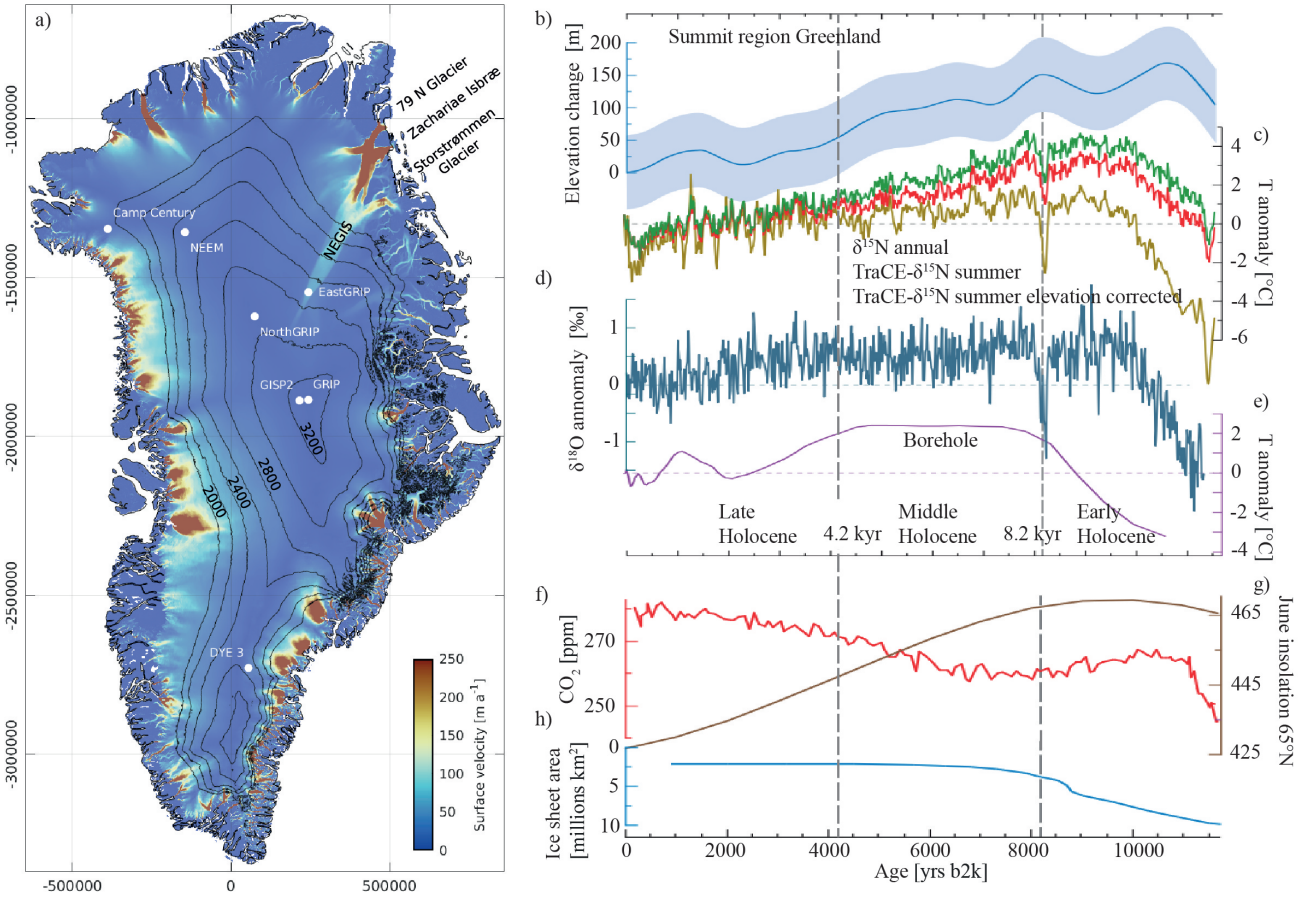

Figure 3. a) Overview map of Greenland, including relevant ice core drill sites and surface velocities from Gerber et al. (2021). b) to h) modified from Axford et al. (2021, fig. 2 and 3e). The vertical dashed lines mark the boundary between early and middle, and middle and late Holocene at 8.2 kyr and 4.2 kyr, respectively. All proxies are shown as anomalies relative to the 1930–1970. b) estimated surface elevation change at Summit (dark blue, Vinther et al., 2009) and uncertainty (faded blue shading, Lecavalier et al., 2013), c) annual δ15N (dark yellow) and summer (red) and elevation-corrected summer (green) Summit temperature anomalies from TraCE-δ15N (Buizert et al., 2018), d) GRIP oxygen isotopes (Rasmussen et al., 2006; Vinther et al., 2006), and e) GRIP borehole temperature reconstruction (Dahl-Jensen et al., 1998). f) Climate forcings and influences including June insolation (Berger and Loutre, 1991), g) atmospheric CO_2 (Monnin et al., 2004), and h) decline of the Laurentide-Innuitian-Cordilleran ice sheet complex (Dalton et al., 2020), y-axis reversed.

Bova et al. (2021) argue that the warm temperatures at the beginning of the Holocene are a bias caused by proxies mostly affected by warmer summer temperatures (fig. 3g), and larger seasonal variations, while the annual mean temperature remained lower and gradually climbed to today's value more or less following atmospheric CO_2 concentrations (fig. 3f).

https://doi.org/10.5194/cp-2021-89
Preprint. Discussion started: 16 July 2021


Climate of the Past Discussions

1.6 The highly dynamic EastGRIP site

The East Greenland Ice Core Project (EastGRIP) ice core, on which we create our melt layer record, is drilled through the Northeast Greenland Ice Stream (NEGIS, fig. 3a). This ice stream flows from the ice divide, between NorthGRIP and the summit area, towards the NNE until it terminates at the coast (Vallelonga et al., 2014). Today's position of the EastGRIP drill site moves with approximately 55 m/yr (Hvidberg et al., 2020), i.e. approximately 15 cm per day.

Gerber et al. (2021) backtrack the location of ice from EastGRIP over time. They show that, e.g., 9000 years old ice was deposited 170 ($\pm$ 17) km further southwest and at a 270 m higher elevation. For their calculations Gerber et al. (2021) use today's ice sheet dimensions, but as Vinther et al. (2009) show, the ice sheet elevation has not been constant over the Holocene (fig. 3b). Vinther et al. (2009) suggest that NEGIS' origin, the area somewhere between the NorthGRIP and GRIP sites, were 150 to 200 m more elevated at the beginning of the Holocene, as compared to today.

The estimate of Gerber et al. (2021) might therefore be rather conservative, and the true elevation change over the past 9000 years may be closer to 400 m. Using the lapse rate estimate of temperatures decreasing by 0.6 to 0.9°C every 100 m of elevation gain (Gardner et al., 2009), we can observe a temperature change at the EastGRIP drill site of 3°C solely by waiting 9000 years, flowing downstream, and ignoring all climatic changes. This underlines that when analyzing EastGRIP-ice we must take into account the spatial variations with time.

https://doi.org/10.5194/cp-2021-89
Preprint. Discussion started: 16 July 2021


Climate of the Past Discussions

2 Methods

2.1 Depth of interest

Our analysis covers the upper approximeteley 1100 m of the EastGRIP ice core. This corresponds to the years 1965 CE to 7601 BCE, i.e. 9566 years, which is a large part of the Holocene (Cohen et al., 2016). We use the age scale provided by Mojtabavi et al. (2020), with a maximum counting error of one to two years. We use the time reference "years before the year 2000 CE" (yrs b2k).

The depth notation in this work refers to the depth below the 2017 ice sheet surface, the year in which ice core drilling began. Ice core processing started 13.75 m below the surface, which corresponds to the year 1965 CE (44 yrs b2k, Mojtabavi et al., 2020). Thus, this is the youngest material available for our analysis.

We terminate our investigation of bubble-free layers at a depth of 1089.64 m, with a very prominent volcanic-ash layer from approximately 9601 yr b2k. This ash layer corresponds to an Icelandic volcano eruption, either from Hekla or Katla (pers. comm. Eliza Cook). The most challenging aspect of this depth is the almost complete transition from air bubbles to clathrates (e.g. Shoji and Langway, 1987; Kipfstuhl et al., 2001; Uchida et al., 2014). With bubbles transforming to clathrates under pressure and thus becoming smaller, the spacing between bubbles increases, and bubble-free layers become increasingly difficult to identify. This bubble-clathrate transformation is not a gradual process but has variable rates for different layers due to their physical properties and the resulting complex crystallization of air hydrates (Weikusat et al., 2015). We use the line scan images to find that the conversion from bubbles to clathrates is fully completed in a depth of 1150 m, but end our analysis 60 m above that depth.

2.2 The Line Scanner and its images

The line scanner is a well-established and powerful tool for high resolution analysis of ice stratigraphy, making use of contrast enhancement by the optical dark-field method. Different devices with similar setups have been used on every deep ice core since the NorthGRIP drilling in 1995 (Svensson et al., 2005; McGwire et al., 2008; Jansen et al., 2016; Faria et al., 2018; Morcillo et al., 2020; Westhoff et al., 2020). The device used at EastGRIP is the second generation Alfred-Wegener-Institute (AWI) line scanner. Images are obtained with a camera moving along the top of a 165 cm long and 3.6 cm thick ice core slab. Two light sources illuminate the polished ice core slab at an angle from below (for details consult Svensson et al., 2005; Westhoff et al., 2020).

The appearance of line scan images is substantially different from firn to ice (fig. 4 left and right, respectively). In firn and snow, the bright sections of the image represent the solid parts, such as snow crystals or ice layers. Dark sections of the image represent voids, i.e. air. When firn has been compressed to ice, the appearance of features is inverted: ice now appears dark and bubbles, i.e. air, are now represented by bright pixels. This inversion of appearance is caused by firn-grains being non-transparent, thus reflecting light. Ice on the other hand is transparent and allows light to travel through without any reflections, thus a dark field below the ice core slab is imaged. Bubbles appear bright, as their rounded ice-air interface offers perfect conditions for light scattering in all directions.

https://doi.org/10.5194/cp-2021-89
Preprint. Discussion started: 16 July 2021

Climate of the Past Discussions
Open Access
EGU

170 The firn-ice transition is situated around 70 m depth (e.g. Buizert et al., 2012), so the largest part of our investigation is conducted on ice with bubbles, where bubble-free layers are easy to identify (e.g. fig. 4d).

2.3 Types of events

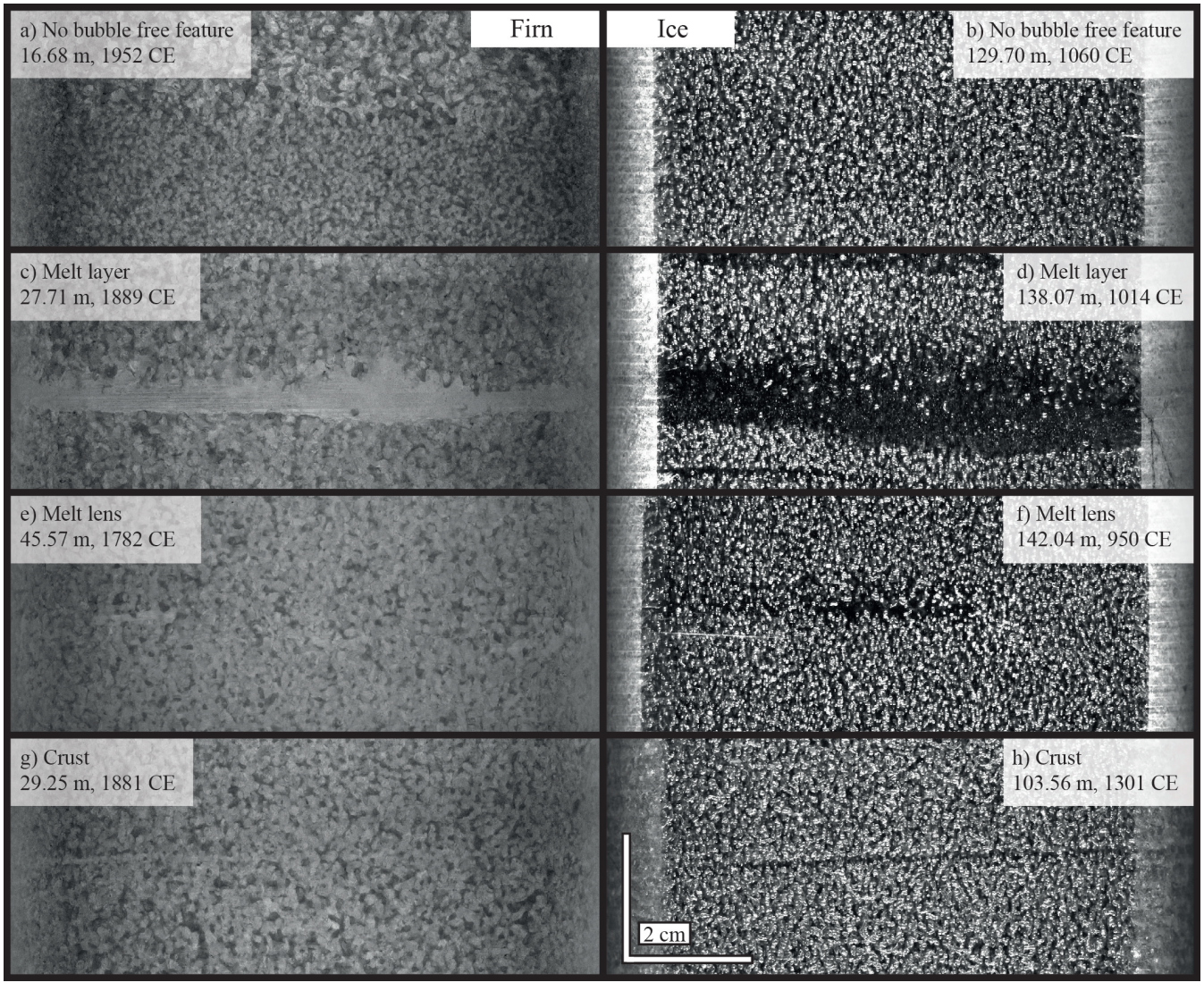

Figure 4. The appearance of different structures in line scan images in firn (left) and ice (right). a,b) Typical examples of appearance of firn and ice. c,d) Bubble-free layers interpreted as melt layers. These are continuous horizontally across the ice core. e,f) Bubble-free lenses interpreted as melt lenses, which are discontinuous patches mostly with a horizontal elongation. g,h) Very thin and straight bubble-free layers with sharp edges. These structures are hard to see in line scan images and are interpreted as crusts, the result of surface hardening by the wind.

https://doi.org/10.5194/cp-2021-89
Preprint. Discussion started: 16 July 2021


Climate of the Past Discussions

In the upper 1100 m of the EastGRIP ice core the majority of the ice contains bubbles, and thus the "normal" appearance of firn and ice (fig. 4a and b). Firn and ice can be bubble-free for two reasons: either snow melted and refroze close to the surface, creating a melt layer or lens, or a surface hardening took place e.g. by wind which forms hard (wind-)crusts. On this basis we define three types of bubble-free features: melt layers (fig. 4c,d), melt lenses (fig. 4e,f), and crusts (fig. 4g,h). Within our three categories, we note the certainty of our labeling as either "certain" or "uncertain". We add a fourth category for features that hint to bubble-free layers but are not completely distinguishable, these can be considered "very uncertain".
We define the different types below:

- Melt layers are in general continuous features ranging across the entire horizontal core width. The melt layer thickness can vary within one layer, but we define, that it should always be greater than one to two millimeter ($1\ mm = 18.6\ pixels$). They can have sharp edges (fig. 4c bottom left) or smooth edges, where bubbles are within the melt layer (fig. 4d top edge).

- Melt lenses have the same appearance as melt layers, yet of smaller dimensions and not continuous across the width of the core. The definition of layer and lens is therefore determined by the core diameter, which is approximately 10 cm in the EastGRIP ice core. Lenses can have a more rounded shape, yet in general, they show an elongation along the horizontal.

- Crusts are very thin bubble-free layers, around one millimeter, and in general continuous from one side of the core to the other. They have a sharp border to the bubbles around them. These thin layers can be identified reasonably well and distinguished from melt layers in the upper 250 m. Yet as thinning of layers proceeds, a distinction is no longer possible. We, therefore, assume that below 250 m, all layers with the appearance of crusts, are actually thinned melt layers. Thinning would be influential to such a degree that crusts are eventually no longer detectable using line scan images.

2.4 Core breaks and the brittle zone

Core breaks influence the counting of melt layers and lenses. Core breaks are fractures in the core, mainly occurring for two reasons: either from breaking the ice core free at the bottom of the borehole (see Westhoff et al., 2020), or from fractures in the brittle-zone ice (Neff, 2014).

- The drilling-related core-breaks are usually approximately horizontal. During smooth drilling operations and good ice quality, core breaks occur every few meters, depending on the length of the core barrel chamber which is implemented in the deployed drilling system.

- In the brittle zone, a zone where the internal pressure of the trapped air bubbles is very high and exceeds the tensile strength of the ice core, the ice core samples will break up and sometimes even explode. This is an effect of pressure-temperature relaxation after core recovery at the surface. Core breaks in the brittle-zone breaks could have any orientation and thus, tend to run diagonally across the core and the line scan image.

https://doi.org/10.5194/cp-2021-89
Preprint. Discussion started: 16 July 2021

Climate of the Past Discussions

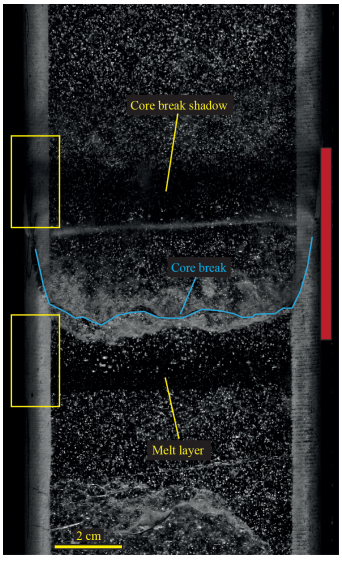

Figure 5. A core break casting a shadow and a melt layer have a very similar appearance in the line scan images. A distinction is made first by the proximity to the break, and then by differences of brightness along the ice core's round drilling edge (yellow boxes). Core break shadows darken the edge of a sample. Minimum section not suited for analysis is indicated by red bar.

Here we want to credit the work of the drill team and the careful logging team, as the brittle zone is extremely difficult to drill and to handle. Even though these core losses due to breaks are high, such a great core quality, as drilled at EastGRIP, has not been achieved in any previous Greenlandic ice core. This gives us the unique chance to perform an analysis in the brittle zone, and quantify the effects of core breaks.

During line scanning, light is introduced at an angle from below the core slab. As core breaks usually have a rough break-surface, then a gap and another rough break-surface, the light intensity will drop when crossing the void. This intensity loss casts shadows on either side of the core breaks. These shadows greatly depend on the geometry of the core break, yet always appear in some form. These shadows can easily be mistaken for a bubble-free layer and fig. 5 is a rare occasion (one of two in total) where a melt layer is very close to a break and distinguishable from it. The main difference is that a core break casts a shadow on the edge of the core slab, while the edge remains at a constant brightness in the presence of a melt layer (yellow boxes in fig. 5).

To account for this difficulty, features close to core breaks are in general disregarded. This implies, that the more core breaks we have, the more bubble-free events we may miss and the more we underestimate the number of events. It is, therefore, necessary to obtain an overview of core breaks throughout the depth of interest. We estimate the chance of missing a bubble-free event by assuming a 4 cm-sample loss for each break. In general, a shadow is cast 1.5 cm to either side of the break and the break itself disturbs the image across at least 1 cm, adding up to 4 cm in total (fig. 5, red bar).

https://doi.org/10.5194/cp-2021-89
Preprint. Discussion started: 16 July 2021


Climate of the Past Discussions

2.5 Data acquisition

The data were collected in a semi-automated fashion using Matlab. We run a script, which divides the line scan image (length 165 cm) into ten equal sections, with two centimeters overlap. Thus, we display 16.5 (+ 2) cm of the core at a time. We display three different color maps: a "hot" map, a "cool" map of the inverted image, and the original grayscale line scan image. Using a tool that records pixel coordinates by clicking on the image, we select the layers of interest. The position of the layer is then immediately converted to depth using

$$depth[m] = ((bagNumber * 0.55) - 0.55) + (pixels/(186 * 100)). \quad (1)$$

A bag is the standard unit in ice coring samples, corresponding to 55 cm. $BagNumber$ refers to the line scan bag number, where only every third bag is listed, meaning one sample (165 cm) corresponds to three bags (55 cm each). We convert pixels to depth, using the value $1cm = 186px$. This means that the depth is referenced to the top of every third bag, not to every bag as is the standard for most other methods. For melt layers we record the upper and lower boundary, for all other features we only record the center value for depth. We did the analysis twice to minimize operator errors and mismatches between were reassessed.

https://doi.org/10.5194/cp-2021-89
Preprint. Discussion started: 16 July 2021

Climate of the Past Discussions

3 Results

3.1 Bubble-free events

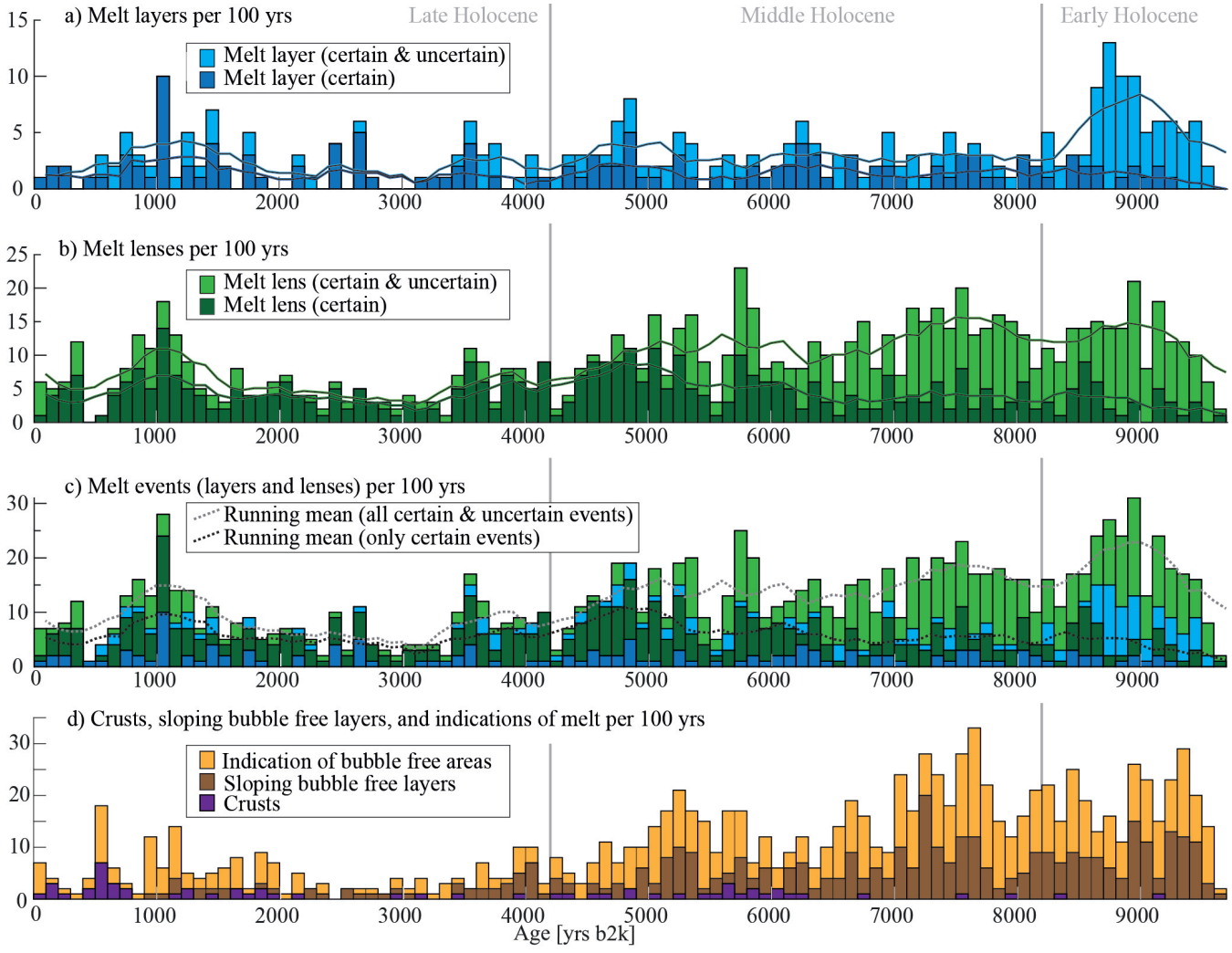

Figure 6. Frequency of bubble-free layers and lenses per century throughout the last 9700 years in the EastGRIP ice core. Running means are shown as solid lines. a) melt layers (dark blue) and uncertain melt layers (light blue), b) melt lenses (dark green) and uncertain melt lenses (light green), c) melt events, i.e., stack of panels a) and b), including their uncertainties. d) indications of bubble-free areas (orange), which are very uncertain melt layers and -lenses that only hint to bubble-free areas. Sloping bubble-free layers (brown) with a tilt of more than 10 degrees from horizontal, which are in general very thin and not always continuous. Crusts (purple) are only certain/clearly identifiable in the last 2000 years (upper 250 m). Note that the bar representing the period from 0 to 100 yrs b2k only represents 56 years, and not 100 like the other bars, as our analysis only begins in 1956 CE.

https://doi.org/10.5194/cp-2021-89
Preprint. Discussion started: 16 July 2021


Climate of the Past Discussions

We find 561 melt events throughout the last 9700 years in the EastGRIP record (fig. 6c), which can be separated into 137 melt layers (fig. 6a) and 424 melt lenses (fig. 6b). Melt lenses are thus almost three times more frequent and represent smaller, more local melt events. We find another 622 events where we could not determine with full certainty if these are layers or lenses. Of these, there are 157 uncertain melt layers and 465 uncertain melt lenses. We remind the reader of the three groups of melt events: certain, uncertain, and very uncertain (also labeled as: indication of bubble free areas), which describe how confident we are in having detected a bubble free layer.

Both melt lenses and layers follow the same trend and are most abundant during the same periods, with an increase towards the early Holocene. We find very few or no melt layers around the years 500, 2000, and 3000 b2k, and also melt lenses are less frequent. We find many certain melt events (dark blue and dark green in fig. 6), around the years 1000, 3500 to 4000, 4500 to 5000, and around 6000 b2k. Fewer in number, but still outstanding, are many melt events occurring between 7500 and 8000 yrs b2k.

Events older than 9000 years become difficult to detect due to progressive bubble to clathrate transformation, therefore values gradually decrease. Also, we do not capture the most recent years, younger than 44 yrs b2k (1956 CE). Therefore the bar representing the period from 0 to 100 yrs b2k only represents 56 years, and not 100 like the other bars (fig. 6).

Other than melt events, we find crusts, sloping bubble-free layers, and indications of melt events (fig. 6d). In total, we find 60 crusts (purple in fig. 6d), of which we are certain about 17. These certain crusts are all in the last 2000 years, i.e. the upper 250 m. Crusts found below this depth are classified as uncertain and were added as uncertain melt layers (see "types of events" section). We find 410 cases of sloping bubble-free layers, mainly in a depth below 600 m (approximately 5000 yrs b2k). These bubble-free layers with an inclination over 10° will be discussed later as it is not clear if they are a climatic signal or of different nature. We also find 579 cases where the line scan images hint at an area or layer without bubbles, but cannot be seen with full certainty. These could represent warm summer days, on which small amounts of surface melt occur, yet not sufficient to classify as melting. These small amount of water on the air-ice interfaces can cause a change in the porosity of the firn. Dash et al. (2006) describe these as enhanced pre-melting and discuss incomplete vs. complete surface melting. These pre-melt events are hard to identify in line scan images, or even under a microscope, and only become visible when comparing the brightness changes over a long section ($> 10cm$). We, therefore, classify these brightness changes as "very uncertain melt layers". They are added to the overview for the sake of completeness and might be useful for comparison to other methods (e.g. Morris et al., in prep.).

3.2 Melt layer thickness

For the 137 certain melt layers, we have also documented their thickness (M_0, fig. 7). The layer thickness is shown by the yellow, orange, and red bars, and to distinguish events within a short period, the thickness is indicated by circles. We distinguish between the measured thickness (M_0, open circles, fig. 7a and b) and the layer thickness corrected for thinning (M, filled circles, fig. 7b and c) for which we use the thinning function from Gerber et al. (2021, fig. 7d). Here we must keep in mind that the thinning is an average of all layers, derived from radar data. It is thus an upper limit assumption for the thinning of melt layers, which are more dense, due to the lack of bubbles, and should therefore thin less than the surrounding ice.

https://doi.org/10.5194/cp-2021-89
Preprint. Discussion started: 16 July 2021

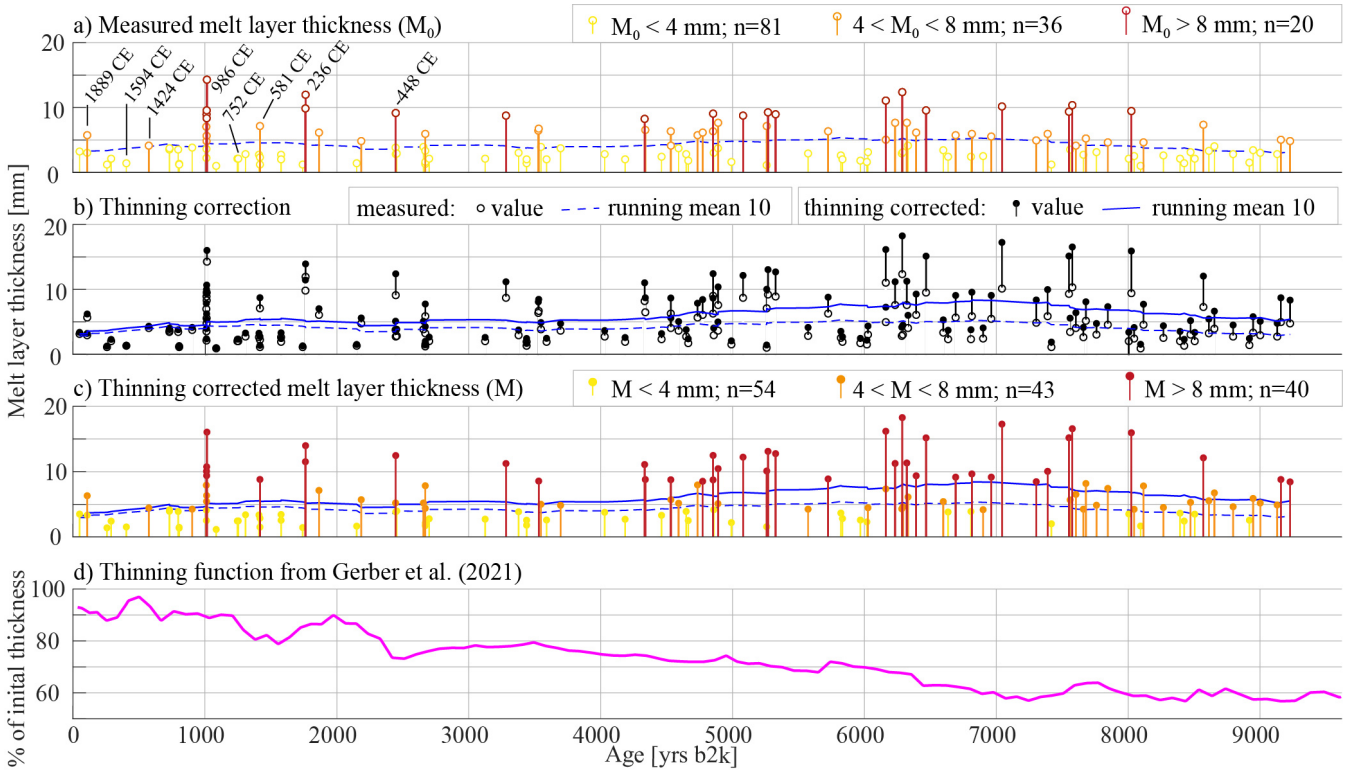

Figure 7. Measured (M_0, panel a) and thinning-corrected (M, panel c) melt layer thickness shown with open and filled circles respectively. Running mean over 10 events with dashed (measured) and solid blue line (thinning-corrected). Individual correction for thinning (b) using the thinning function from Gerber et al. (2021) shown in d). Yellow, orange, and red bars with circles indicate melt layers with a thickness smaller than 4 mm, between 4 and 8 mm, and greater than 8 mm, respectively. Labeled in panel a) are events later compared to tree rings with ages in [CE] notation.

Thin melt layers ($M < 4mm$, yellow) are found throughout the Holocene, yet seem to be more abundant in the late Holocene (last 4200 years before today). Thick melt layers ($M > 8mm$, red) become more frequent further back in time. This trend is also highlighted by the blue curves, representing the running means. The thinning-corrected running mean (solid blue line, fig. 7b,c) points to an average melt layer thickness of around 5 mm for the past 4500 years. Going back further in time, we see a gradual increase in melt layer-thickness in ice older than 4500 years (fig. 7c), peaking at an average thickness of 8 mm around 6500 to 7000 yrs b2k (solid blue line). In events older than 7000 years, the mean gradually drops and the last melt layer found is in ice deposited 9235 yrs b2k.

We expect to miss thinner melt layers the further back we go in time, which is represented by our results (fig. 7c) where we only find seven thin melt layers ($M < 4mm$, yellow) between 7000 and 9700 yrs b2k. In the same period we find 15 medium ($4mm < M < 8mm$, orange) and nine thick melt layers ($M > 8mm$, red). Assuming we miss thin layers but not thicker ones, we would expect a continuous increase in average melt layer thickness. Yet this average gradually drops below 7500 yrs while

https://doi.org/10.5194/cp-2021-89
Preprint. Discussion started: 16 July 2021

Climate of the Past Discussions
Open Access
EGU

we approach Holocene Climatic Optimum (HCO). A possible reason for this gradual drop could be the two cooling events 8200 and 9300 years ago (Thomas et al., 2007; Rasmussen et al., 2007).

The thickest melt layers found in our record lay between 6100 and 6500 yrs b2k (fig. 7c), with thicknesses exceeding 15 mm. Only five other events with such great thicknesses are found, four between 7000 and 8100 yrs b2k and one at 1014 yrs b2k (986 CE). This allocates the majority of thick melt layers to the middle Holocene (Northgrippian Period, Cohen et al., 2016).

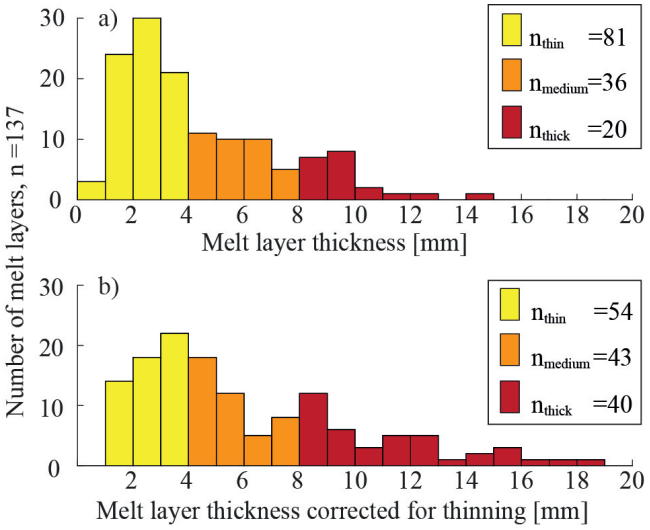

Figure 8. Histogram of melt layer thicknesses with the same color-code as fig. 7. a) measured values, b) corrected for thinning using the thinning function from Gerber et al. (2021).

Over the Holocene, the range of melt layer thicknesses varies between 1 and 14 mm (fig. 8a). Although following the definition, a melt layer cannot be thinner than two millimeters, we find 27 layers below this threshold, before correcting for thinning. These are events that are included for one of two reasons: they vary in thickness and an estimated average was taken or they have the distinct appearance of a melt layer and can clearly be differentiated from a crust. Correcting for thinning removes the layers between zero and one millimeter and provides three categories of similar sizes, with 54, 43, and 40 events per group.

We see that most melt layers ($n = 81$, fig. 8a) are thin melt layers ($M < 4mm$, yellow). Even after correcting for thinning, this remains the same, althought the size of the groups are more equal now (fig. 8b). Thick melt layers ($M > 8mm$, red) remain the fewest, although their number doubles when correcting for thinning. We find 40 thick melt layers in almost 10,000 years, giving an average of one big melt layer in 250 years. On average we find one melt layer every 70 years, but not regularly (compare to fig. 7).

https://doi.org/10.5194/cp-2021-89
Preprint. Discussion started: 16 July 2021

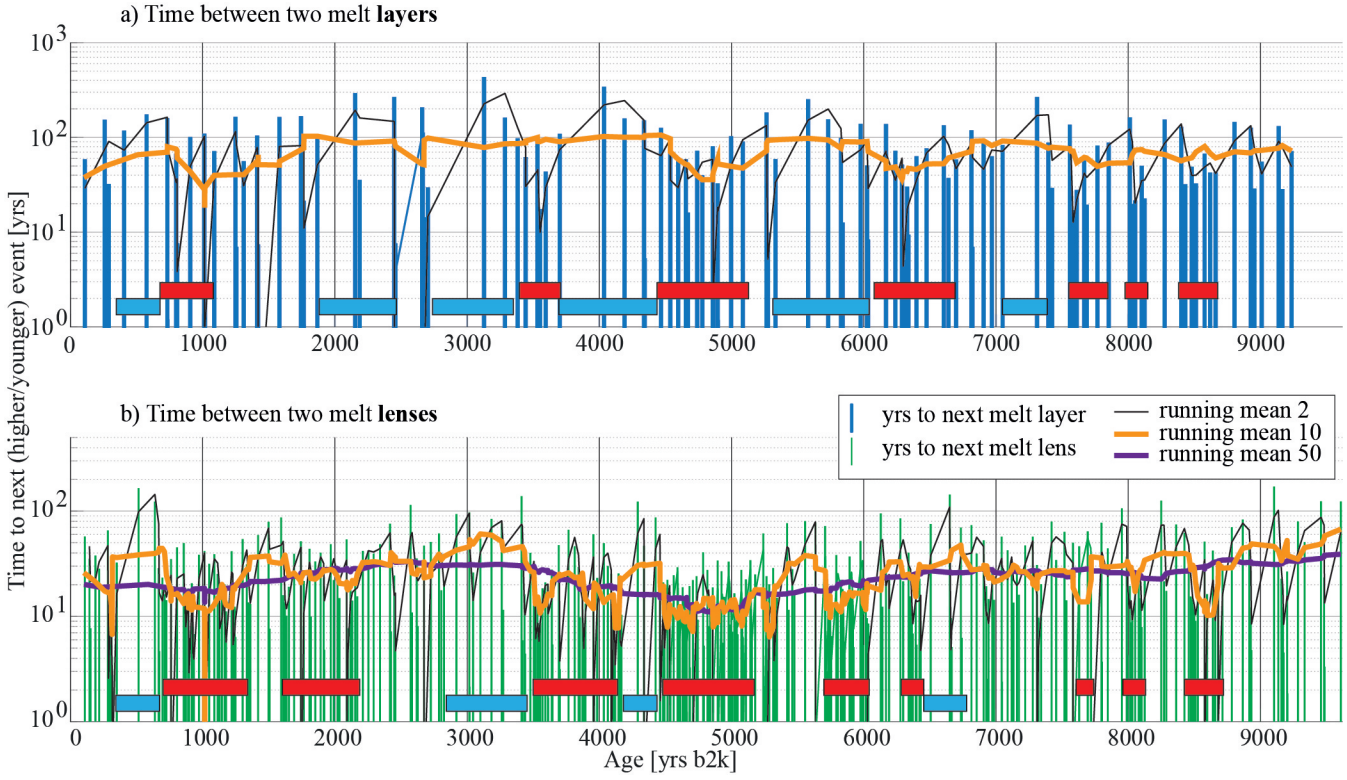

Figure 9. Time from older event to next younger event, a) for 137 melt layers (vertical blue bars) and b) 424 melt lenses (green bars). Different running means (averages with moving window) to visualize long-term variations. Red bars highlight periods with a short spacing between events, and blue bars represent a long spacing.

3.3 Melt event frequency

We analyze the duration between melt layer and melt lenses, representing the time from an older event, to the next younger event (fig. 9). We distinguish between melt layers (blue bars, fig. 9a) and melt lenses (green bars, fig. 9b). Running means for 2, 10, and 50-year events show the long-term variations. Due to melt lenses being approximately three times more frequent, their spacing is much smaller than that of melt layers.

In fig. 9b (melt lenses), around 1000, 3500 to 4000, 4500 to 5500, around 6000, 8000 to 8200, and around 8500 yrs b2k the time between two melt lenses is between 10 to 15 years (orange running mean), therefore very short (red bars). We find a very large spacing (blue bars) of events around 500 yrs b2k, where the spacing exceeds 100 years and in the period from 3000 to 3500 yrs b2k, where the spacing between two melt lenses is around 60 years. Such a large spacing between two melt lens events only becomes visible again in ice older than 9000 years, where bubble-free layers become more difficult to see and we end our analysis.

https://doi.org/10.5194/cp-2021-89
Preprint. Discussion started: 16 July 2021


Climate of the Past Discussions

A similar pattern is also visible in fig. 9a (melt layers), yet with fewer details, as melt layers occur less frequently. Time spans with high melt lens frequencies roughly match periods with high frequencies of melt layers. An outstanding difference is the period from 5800 to 6200 yrs b2k, where the time between two melt lenses is short, but between melt layers it is long. The opposite is visible around 6400 yrs b2k, where the time between two melt layers is short, but long between the lenses.

In both records (fig. 9a and b) we find three shorter time spans around 7800, 8100, and 8500 yrs b2k which have a very short spacing between two events.

The long term trend (fig. 9b, purple line) which is the running mean over 50 events suggests the largest spacing between two events around 3000 yrs b2k with approximately 30 to 35 years and the lowest around 5000 yrs b2k with 12 years spacing. Older than 5000 years the trend gradually increases, showing greater spacing between two melt events, with a small drop around 7500 yrs b2k. The highest value of 35 years between two events is only reached at the very bottom of our analysis depth, older than 9000 years, where the likelihood of missing an event greatly increases.

3.4 Core breaks and their implications

We count core breaks (fig. 10a, orange bars) in the upper 1100 m of the EastGRIP ice core and show the corresponding ages and depths. The running mean over 16.5 meters (fig. 10a, brown line) clearly locates the brittle zone between 650 and 950 m depth. A core break masks four centimeters of a sample (see method section), which is approximately 2.5% of the 165 cm-sample. In the brittle zone, the number of core breaks greatly increases and exceeds three breaks per meter (or five breaks per 165-cm sample). In sections with six core breaks per meter we lose almost 25% of the sample.

As we know the number of melt events per sample, we can estimate the number of events missed due to core break shadows (see methods section). Events per 100 years are shown by vertical bars and the potentially missed melt events, i.e. our core break correction, in orange (fig. 10b, mean values in fig. 10c). The largest corrections are therefore performed in the brittle zone where we add around 25% to the number of melt events. This does not change the overall picture much but shows that we probably underestimate melt events in the time between 6000 and 8000 yrs b2k.

Our correction described above, assumes no correlation between the location of core breaks and melt layers. This correlation could be expected as melt layers might affect the crystal structure or other physical properties of the core. We perform a non quantitative visual inspection and do not find any connection of melt layers weakening, or strengthening, the ice and thus affecting the initiation and location of core breaks in the brittle zone.

3.5 The Final Melt Layer Record

We present a final melt layer record, showing the total amount of melt per century and millenium (fig. 11b and c, respectively). This record is corrected for thinning and for potentially missed layers due to core breaks. For consistency, we cut out layers that are thinner than 1.54 mm. This is the thinnest layer found in the oldest section, with an age of 8101 yrs b2k (fig. 11a, pink circle). We apply the threshold on thinning-corrected layers (fig. 11a, pink line). The layers removed from our record are plotted in black and do not change the overall impression (fig. 11b and c). Melt layers that might have been missed (orange, in fig. 11b,c) mainly lay around the HCO, 6000 to 8000 yrs b2k.

https://doi.org/10.5194/cp-2021-89
Preprint. Discussion started: 16 July 2021

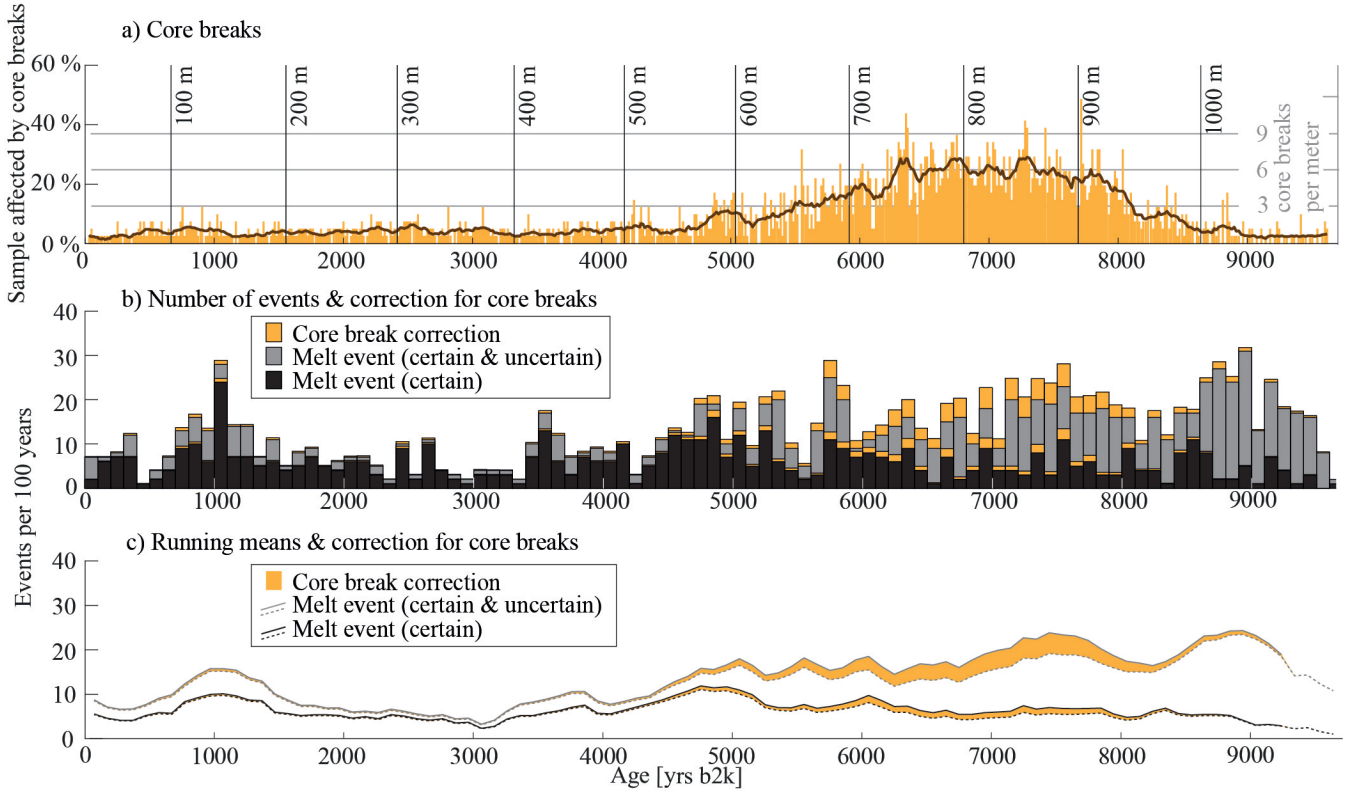

Figure 10. a) Percentage of 165 cm-sample affected by core breaks (orange bars, scale left side), amount of core breaks per meter (orange bars, scale right side), and running mean over 16.5 meters (brown line). The broad peak between 650 and 950 m depth indicates the brittle zone. b) Certain melt events (black) and uncertain melt events (gray) corrected for potentially missed events in proximity of core breaks (orange). c) Running means of melt events, from fig. 6c (dashed lines) and core-break corrected means (solid line).

Millimeters of melt per century (fig. 11b) displays the high variability of melt events, as some centuries do not contain any events. Yet, the running mean (black line) shows distinct spikes, around 4500 to 5000 yrs b2k, 6000 to 6500 yrs b2k and around 7500 yrs b2k. These coincide with the period of the HCO.

The HCO is also pronounced in the amount of melt per millennial (fig. 11c), with a peak in the interval between 6000 and 7000 yrs b2k.

Outstanding in both plots, centuries and millennia, is the peak around 1000 yrs b2k. The melt event from this period, i.e. 1014 yrs b2k or 986 CE, was of such an intensity, that it leaves an unprecedented spike in the melt record of the past 10,000 years. Here, it is important to note, that this is an event confined to a short period over one or a few summers, and not a signal representative for the entire century or millennium.

https://doi.org/10.5194/cp-2021-89
Preprint. Discussion started: 16 July 2021

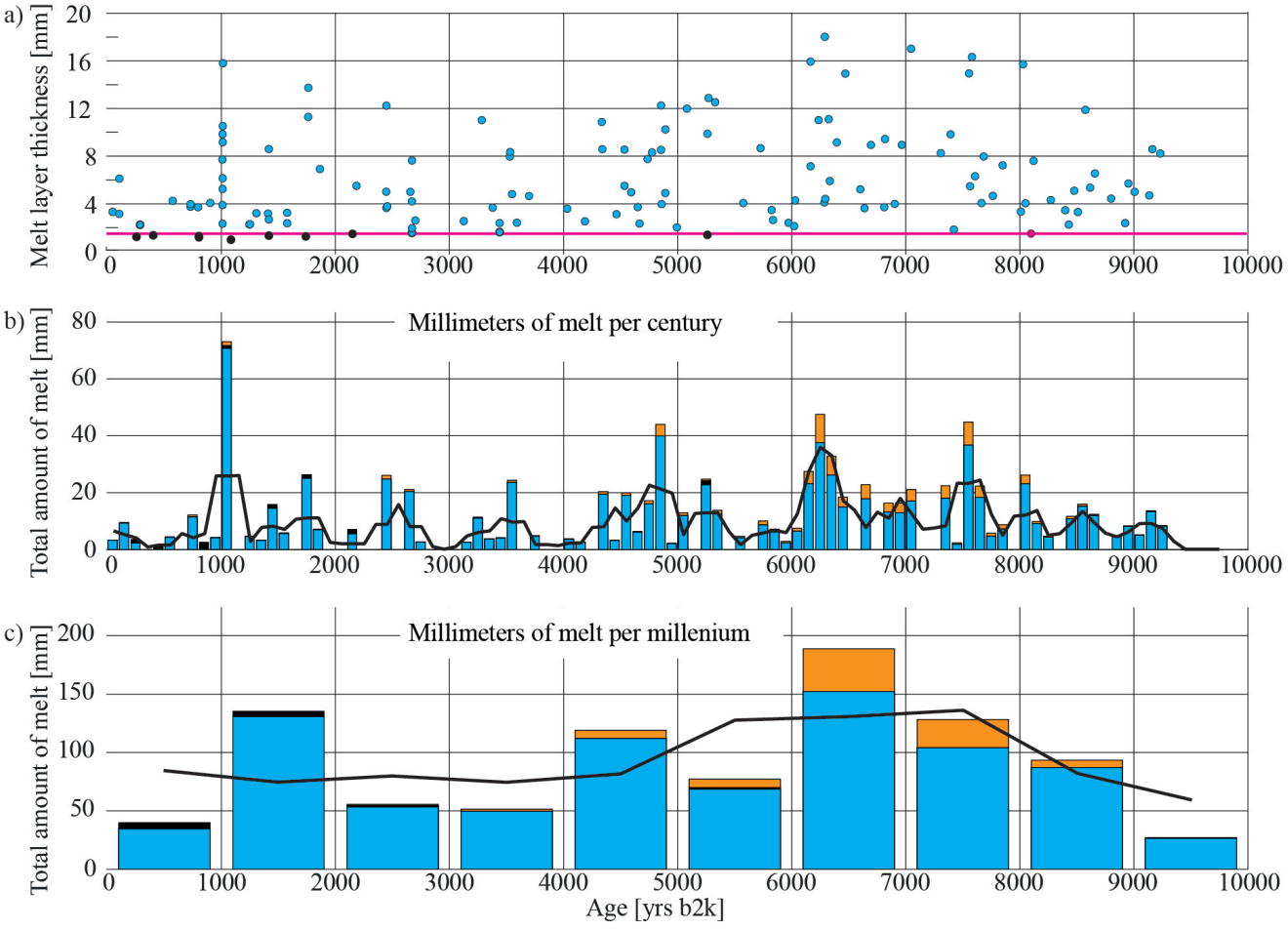

Figure 11. a) thinning corrected melt layer thicknesses (circles). black-colored circles are removed from the record, due to cut off at 1.54 mm (pink circle and line). b/c) Total amount of melt per century/millennial (blue bars, calculated from melt layer thicknesses), potentially missed events due to core breaks (orange), and running mean (black line).

4 Discussion

4.1 The climatic picture of the Holocene derived from melt events

As Axford et al. (2021) describe, there are two possible interpretations of the Greenland Holocene temperature: 1) From a compilation of ice cores, pollen, and marine cores we see a stable temperature with a muted HCO and 2) from ice cap retreat, non-pollen paleoecological evidence from lakes, and offshore marine cores we get a strong HCO and a strong cooling trend until recent years. Bova et al. (2021) suggest that there is no HCO and temperatures gradually increased over the Holocene, but that there are warmer summer temperatures and greater seasonality in the early Holocene.

https://doi.org/10.5194/cp-2021-89
Preprint. Discussion started: 16 July 2021

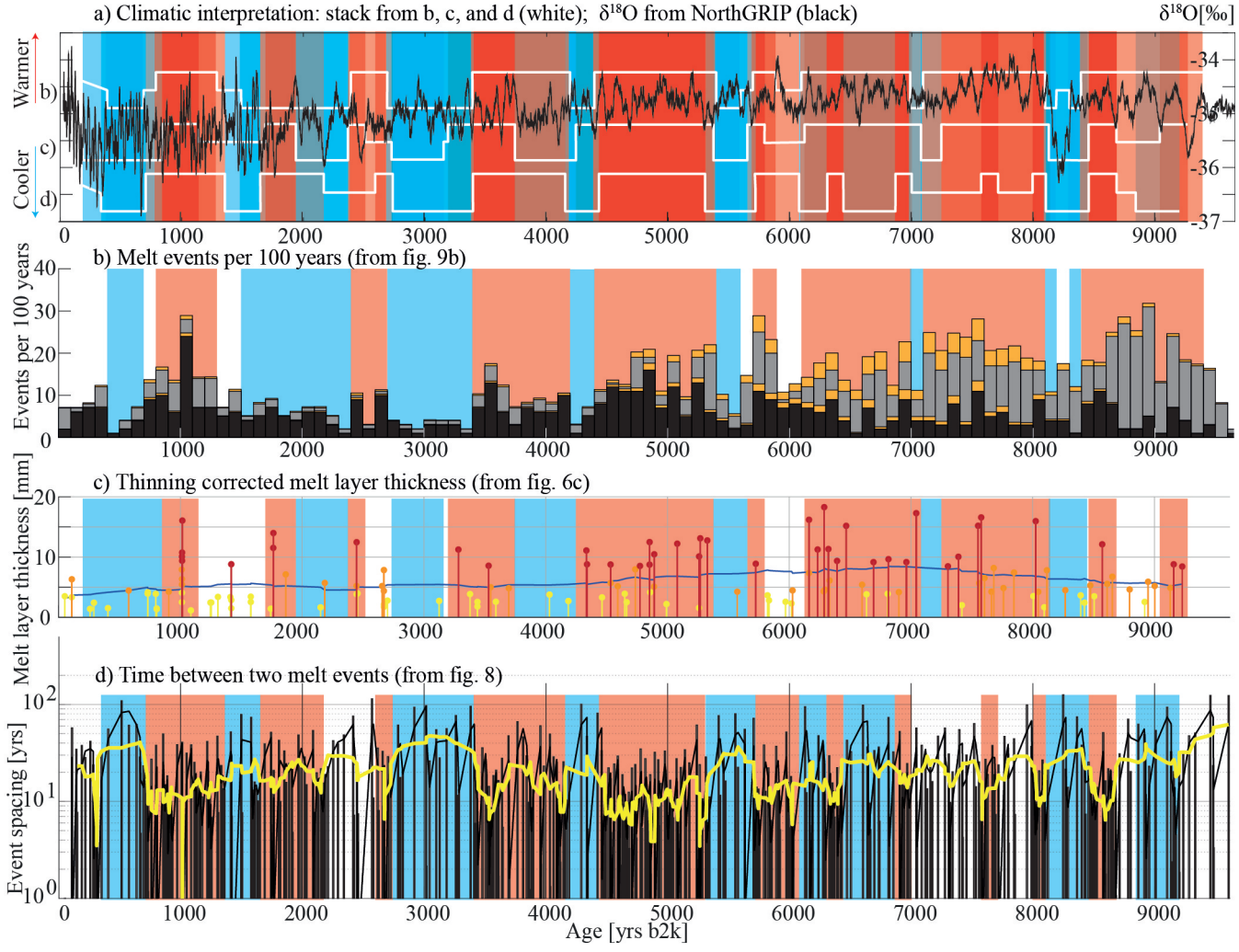

Figure 12. a) A climatic interpretation of melt layer distribution over the Holocene. Without absolute values, red represents warmer periods and blue colder ones. The white lines are a climatic interpretation from b), c), and d) and red and blue shadings are a stack of b), c), and d). Stable Oxygen Isotope ($\delta 18O$) record from NorthGRIP in black (NorthGRIPmembers, 2004). b) melt events per 100 years (fig. 10b) with red shading in periods with many events, and blue in periods with fewer events. c) melt layer thickness (fig. 7c), with red shading in periods with thick melt layers. d) Melt event frequencies (combination of fig. 9a and b), with short time spans between melt events in red and long time spans in blue. Running mean in yellow.

Our climatic interpretation (fig. 12a) is derived from the number of melt events, melt layer thickness, and melt event frequency (fig. 12 b,c, and d respectively). In the central northeastern part of the Greenland ice sheet, i.e. the EastGRIP site, we see strong variations in these melt layer proxies over time, resulting in a fluctuating climate over the past 10,000 years. Yet the overall picture, using all identified melt events, shows a gradual decrease of temperature with the last peak at around

https://doi.org/10.5194/cp-2021-89
Preprint. Discussion started: 16 July 2021


Climate of the Past Discussions

1000 yr before today. We remind the reader that our analysis ends in the year 1956 CE, not covering the most recent events. This climatic interpretation fits well with the generally accepted theory, that summer temperatures decrease throughout the Holocene (e.g. Axford et al., 2021) and also follows the trend of the stalbe water isotopes, a proxy for temperature (fig. 12a). As melt events generally occur during summer, the interpretation also holds for recent results by Bova et al. (2021) that annual temperatures increase and summer temperatures decrease throughout the Holocene.

Our data suggest that the warmest periods in the Holocene are around the year 1000, between 3500 and 4000, between 4500 and 5300, and between 6000 and 8100 yrs b2k. We clearly see the Medieval Warm Period around the year 1000 yrs b2k, identified by a number of melt layers and lenses. Concerning the Roman Warm Period, only the second half (2000 to 1600 yrs b2k) is visible in the number of melt events and the melt layer thickness (fig. 12b and c, respectively), while the full period (between 2250 and 1600 yrs b2k) is represented by melt event frequencies (fig. 12d). Based on fig. 12a, we see the warm HCO from 5800 to 7000 yrs b2k, 7200 to 8100 yrs b2k, and from 8500 to 8700 yrs b2k, with cooler periods in-between.

We find distinct cold periods around the year 500, 3000, 5600, and 8200 b2k. In all our measurements (fig. 12) the 8.2 kyr event (Thomas et al., 2007; Rasmussen et al., 2007) stands out as a period with very few melt events and only one melt layer. Our analysis does not show the 9.3 kyr event, as this is where we lose the signal due to the disappearance of bubbles.

Periods that are neither explicitly warm nor cold, are left with a white shading (fig. 12). This is especially the case for the very recent past, i.e. younger than 100 yrs b2k. In these youngest 100 years of our record, we see a clear increase in the stable water isotope signal (NorthGRIPmembers, 2004, fig. 12a), displaying an increase of temperature over the Greenland ice sheet. This most recent period cannot be covered by our melt layer analysis and we rely on other data sources, e.g., from Steen-Larsen et al. (2011), who suggest that we have five melt events in the past 15 years. These melt events are derived from satellite-based microwaves and their existence in the snowpack is not confirmed, thus must be treated with caution. These 15 events would translate into 33 events per 100 years and would create a peak slightly higher than the one at around 1000 yrs b2k in our record. From here on, we refer to the peak around 1014 years b2k as the 986 CE event.

4.2 Lessons learned from the Coffee Experiment

The coffee experiment was designed as a simple setup to visualize the percolation of melt through the snowpack. Fig. 2a,b show three injection points for cold coffee, as a colored substitute for meltwater, to infiltrate the snow. Vertical melt pipes remain mostly invisible, but the horizontal expansion of the coffee into layers and lenses is very pronounced. It is worth noting that this represents one event, which creates multiple layers in the snowpack. Furthermore, these melt layers are not at the surface, but penetrate 40 cm deep. It is also easily visible, that melt layers from the same event (coffee injection) can appear very different, despite the fact they are only 20 cm apart, i.e. on either side of the trench wall (compare fig. 2a and b). Having multiple melt layers and lenses in such close vertical proximity thus indicates a rain event on the ice sheet. This experiment is therefore more a simulation of a rain event, rather than a small melt event.

Such a rain event has been observed, e.g. in the year 2012 at NEEM, where the occurrence of melt layers in depth over the span of the warm event were documented (fig. 2c). Atmospheric temperatures exceeded 0 °C on four days and melt layers formed up to a depth of 140 cm below surface. Over the duration of this warm event melt layers formed in deeper depths every

https://doi.org/10.5194/cp-2021-89
Preprint. Discussion started: 16 July 2021


Climate of the Past Discussions

day, also related to a gradual warming of the snow pack. It therefore seems like the length of a warm event influences the percolation depth of melt layers.

We can find such a past rain event in the EastGRIP ice core around the year 986 CE, or slightly after, in a depth of 138.05 m (fig. 2d, bag 252). Here we count nine melt layers and 12 melt lenses over 60 cm, which cover five years. Seven of these melt layers, and approximately three years, are visible in fig. 2d, one more melt layer is just above, and one just below the selected image. These melt layers and lenses are the huge spike around the year 1000 CE in the figures (e.g. fig. 6), and may not represent nine separate events, but could have been created in one single event. We can assume that the rainwater percolated 1.5 m deep into the snowpack and left nine melt layers. All of these layers thus may have formed within a few days, similar to the 2012 warm event at NEEM (fig. 2c). The depth of 1.5 m roughly covers five years making this assumption feasible.

Rain events are rare on the Greenland ice sheet and the 986 CE event stands out as a huge melt event with probably very high surface temperatures and rain. It is also worth noting, that the 1889 CE melt event, which is present in most areas and ice cores across Greenland and therefore considered a big event, consists of only two melt layers, and must therefore not have been as intense as the 986 CE event. The only melt event that can get close to the 968 CE event, yet with significantly thinner layers, happened around the year 675 BCE (2675 yrs b2k and 328 m depth) with four melt layers and three melt lenses within the stratigraphy of one year. Thus, these events are rare in Greenland, even over the course of the entire Holocene.

4.3 Integrity of our (and other) melt layer records

"How likely is it to miss an event?" This question can be addressed in two ways: either by missing an event in our analysis or because it is not there in the first place. As we also include events with uncertainty, we greatly reduce the chance to miss an event during our analysis. A wrong labeling can happen, as we only have a 2D image of the ice core, meaning if a melt lens is behind bubbles it becomes hard to see in our images, and will probably end up in an uncertain category or be missed. The prominent and big events (fig. 7, orange and red) will not be missed with our analysis. These structures are too obvious in the line scan images and, as stated before, our analysis was done twice, minimizing operator errors.

On the other hand, we can miss bubble-free layers in our ice core record if they are not there. Studies such as Keegan et al. (2014), Schaller (2018), Fegyveresi et al. (2018), or Taranczewski et al. (2019) show the high spatial variability of melt lenses in trenches or shallow cores. While the spatial distribution of a melt lens or a layer is not homogeneous over larger areas, our ice core with a diameter of 10 cm is a very small sample of the ice column. Also, the coffee experiment (fig. 2) shows that depending on where one would take an ice core with a diameter of 10 cm, the appearance of melt layers and lenses would be very heterogeneous. What has also been shown (e.g. Keegan et al., 2014) is that big melt events, such as the 1889 event are visible in most shallow cores and snowpits and thus prove a widespread distribution. For bigger events, we can therefore assume that our analysis is representative of the largest part of Northern Greenland, while smaller events might be restricted to local areas.

Another problem with interpreting melt layers is shown in the snowpit sampling during the 2012 melt event at NEEM (fig. 1 and fig. 2c). Melt layers are not deposited in exactly the layer with the corresponding snow-age of that day or year, but further below. The signal of a melt layer is therefore parasitic in snow, later firn and ice. The melt layer originates from a different

https://doi.org/10.5194/cp-2021-89
Preprint. Discussion started: 16 July 2021

Climate of the Past Discussions
Open Access
EGU

time of the year, or sometimes even a different year. Pfeffer and Humphrey (1998) perform a very detailed study on meltwater infiltration into the snowpack which highlights this effect. Therefore, interpretations of melt events on an annual time scale should be handled with care, as the melt layer-age does not necessarily match the ice-age. This effect can be neglected on the decadal and upwards resolution.

4.4 A first attempt to interpret sloping bubble-free layers

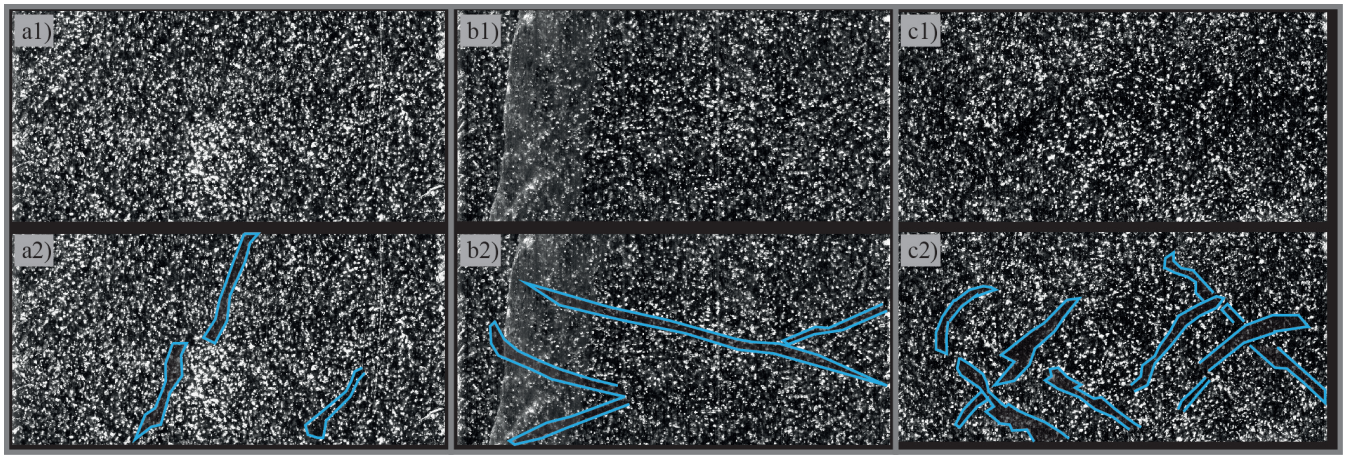

Figure 13. Top row: Line scan images, bottom row: same image as top row, with highlighted sloping bubble-free layers. a) 459.60 m, 3840 yrs b2k, very steep structures, melt pipe-like appearance. b) 696.26 m, 5886 yrs b2k, continuous bubble-free structure appear as a set of conjugate deformation bands. c) 998.73 m, 8625 yrs b2k, many sloping bubble-free layers all at angles around 45°.

Sloping bubble-free layers (fig. 13) become more frequent in the lower half of our investigation depth, i.e. below 600 m, or older than 5000 yrs b2k (fig. 6d). These are layers that have a tilt greater than 10° from horizontal, mostly between 30° and 60° (fig. 13). In general, they are discontinuous, giving them the appearance of a lens, rather than a layer. These thin and hard-to-see structures are very dependent on which plane, by chance, was cut to produce the 2D line scan image (Westhoff et al., 2020). A layer like in fig. 13 can easily be missed if it is located just a few millimeters below the surface.

While it is difficult to say what these layers are, it is possible to exclude some options: they are not the leftovers of sloping surface structures, such as sastrugi. Even a 45° surface-slope would appear relatively flat when being thinned in vertical and stretched out in the horizontal direction during the process of metamorphism from snow to firn to ice. Waddington et al. (2001) describe this “flattening” effect for folds, saying that sloping and folded layers in lower parts of the ice column are not leftovers from surface structures. This assumption is also applicable to our sloping layers.

Figure 13 a) is an almost vertical structure and thus could be a melt pipe (a vertical structure through which meltwater percolates into the snowpack). This explanation makes sense, yet fails to explain why we only see these structures in great depths. The same explanation could also be used for fig. 13 b) and c) assuming these are former almost-vertical melt pipe

https://doi.org/10.5194/cp-2021-89
Preprint. Discussion started: 16 July 2021


Climate of the Past Discussions

structures, that get bent to the side due to vertical thinning and horizontal stretching (pure shear) of the ice with depth. Again, this theory fails to explain why we do not find vertical structures in the upper half of our depth of interest.

Sloping layers at around 15° and 45°, fig. 13 b) and c) respectively, appear to be sets of conjugate bands. This opens the door for a different interpretation: they could be the result of rheology. Steinbach et al. (2016) and Llorens et al. (2017) show sets of conjugate shear bands as a result of pure shear in ice in their numerical simulations. In nature so far, all sloping layers allocated to deformation, are the result of simple shear (e.g. Alley et al., 1997; Jansen et al., 2016) and not pure shear. A problem with this interpretation is that we expect shear bands where ice is softer, thus brighter, and containing more bubbles. Our results show that these shear bands appear in dark, bubble-free layers, contradicting the established theory. While discussing these deformation structures in detail is beyond the scope of this work, it is worth mentioning these for future investigations.

4.5 Comparison to other melt layer records

4.5.1 GISP2

To compare our work, we use the only other melt layer record from a central Greenland ice core covering large parts of the Holocene. Alley and Anandakrishnan (1995) analyzed the GISP2 ice core using visual inspection and to some degree photography, the state-of-the-art method at that time. On average they find one melt event every 153 years. We find one melt event every 17.3 years in the EastGRIP ice core (561 melt events in total, fig. 6c). We can dedicate our increase in finding melt events by a factor of 10 to the better optical methods nowadays.

The sites GISP2 (Alley and Anandakrishnan, 1995) and EastGRIP (this work) are both in a central region on the Greenland ice sheet and the ice recovered at EastGRIP, inside the NEGIS, originates upstream from the GRIP and GISP2 area (Gerber et al., 2021). While ice flows downstream the site elevation decreases and temperature gradually increases (see introduction). For the early Holocene, we can therefore assume the records must be in some way similar, but the number of events should gradually increase towards present day. This holds, as the GISP2 record has a very pronounced HCO (between 6000 and 8000 yrs b2k), while our record (of certain events, fig. 6c, dark colors) shows melt events to be slightly more evenly distributed over the past 10,000 years. When we include uncertain events (fig. 6c, bright colors), the GISP2 and EastGRIP records are very similar and their peaks align well.

At site A, Greenland (70,8 °N, 36,0 °W, 3145 m), south east of GISP2 and approximetley 2 °C warmer, Alley and Koci (1988) find nine melt events in the last 300 years. This relates to one event every 33 years at a site which is two degrees warmer than GISP2. Alley and Anandakrishnan (1995) argue that a value of one event per 33 years relates to a temperature increase of two degrees, compared to one event every 153 years. As this value was not reached in their record, they assume the temperature variations throughout the Holocene must have been below two degrees.

If an increase of melt layers by a factor of five (from one event every 153 years to one every 33 years, see paragraph above) is related to a temperature increase of two degrees, then the Greenland ice sheet is a highly vulnerable system (Boers and Rypdal, 2021). Furthermore, changes in temperature of around one degree could cause events with significantly thicker melt layers (fig. 7) and more frequent events (fig. 9). We can therefore assume that a change of annual temperature of one

https://doi.org/10.5194/cp-2021-89
Preprint. Discussion started: 16 July 2021

480 degree is highly effective. This change of temperature can be caused by a change of elevation of the Greenland ice sheet (see introduction). Lowering the central region of the ice sheet by just 150 m would easily create this one degree, as temperature rises by approximately 0.6 to 0.9 °C per 100 m decrease in elevation (Gardner et al., 2009). It can also be caused by a change of the global climate.

4.5.2 RECAP ice core

485 Another available, but not yet reviewed, melt layer record is assembled by Taranczewski et al. (2019) of the RECAP ice core. The authors present a melt layer record for the last 10,000 years on Renland, eastern Greenland. In this ice core, the Holocene covers 533 of the 584 meters of total core length (Simonsen et al., 2019). As the Holocene ice reaches almost to bedrock, it is subjected to high amounts of thinning in the bottom parts. As thinning equally affects bubble-free ice and bubbly ice (for ice, no study has shown the opposite so far), the signal is lost at a much shallower depth than at EastGRIP or GISP2. The RECAP
490 record, therefore, provides a very robust melt layer record for the late Holocene (past 4200 years before today), but not the middle and early Holocene.

Taranczewski et al. (2019) find a broad peak of melt events around 4000 years b2k, which is not visible in the GISP2 (Alley and Anandakrishnan, 1995) or EastGRIP (this study) melt layer record. The RECAP melt layer record is thus likely a regional record of Eastern Greenland, but not fully comparable with the central ice sheet.

495 4.6 Melt layers and Northern Hemisphere tree rings

A comparison between melt events and Northern Hemisphere temperatures was made by using the tree ring composite record (N-Tree) presented by Sigl et al. (2015). The record comprises tree-ring growth anomalies from five different locations across the Northern Hemisphere, where temperature is the limiting factor to growth. The N-Tree record is presented on its independent annual ring-width timescale (NS1-2011), carrying no uncertainty according to Sigl et al. (2015). The individual records from
500 northern locations in Finland, Sweden, Siberia, Central Europe, and USA almost always overlap, providing a composite average of the tree growth in response to temperature.

For the comparison to the tree ring data, we plot EastGRIP on the NS1-2011 timescale. For this, we interpolate EastGRIP depths to the GICC05 chronology (Mojtabavi et al., 2020) and then translate these ages to the more recent chronology (NS1-2011). The ages in CE, as the names of selected events (fig. 14b to h), are from the GICC05 timescale, as this is used throughout
505 our study. We verified good alignment of EastGRIP and N-Tree data as many volcanic eruptions align to drastic cooling events within one to two years (Sinnl et al., in prep.).

We evaluated the age offset of seven melt events (see also fig. 7a) to the highest peak in the tree ring record, within a ±6-year window around the melt event (fig. 14b to h). Melt events lay very close to a tree-ring peak, in most cases within the same year. Two events show an offset of four to five years to the highest peak within the ±6-year window (E4 and E6, fig. 14e and g,
510 respectively). We find a slightly smaller peak around the same year as the melt layers. Thus, we attribute this offset to incorrect peak assignment. All highlighted events (black boxes, E1 to E7) have at least one tree ring peak (warm anomaly) in very close

https://doi.org/10.5194/cp-2021-89
Preprint. Discussion started: 16 July 2021

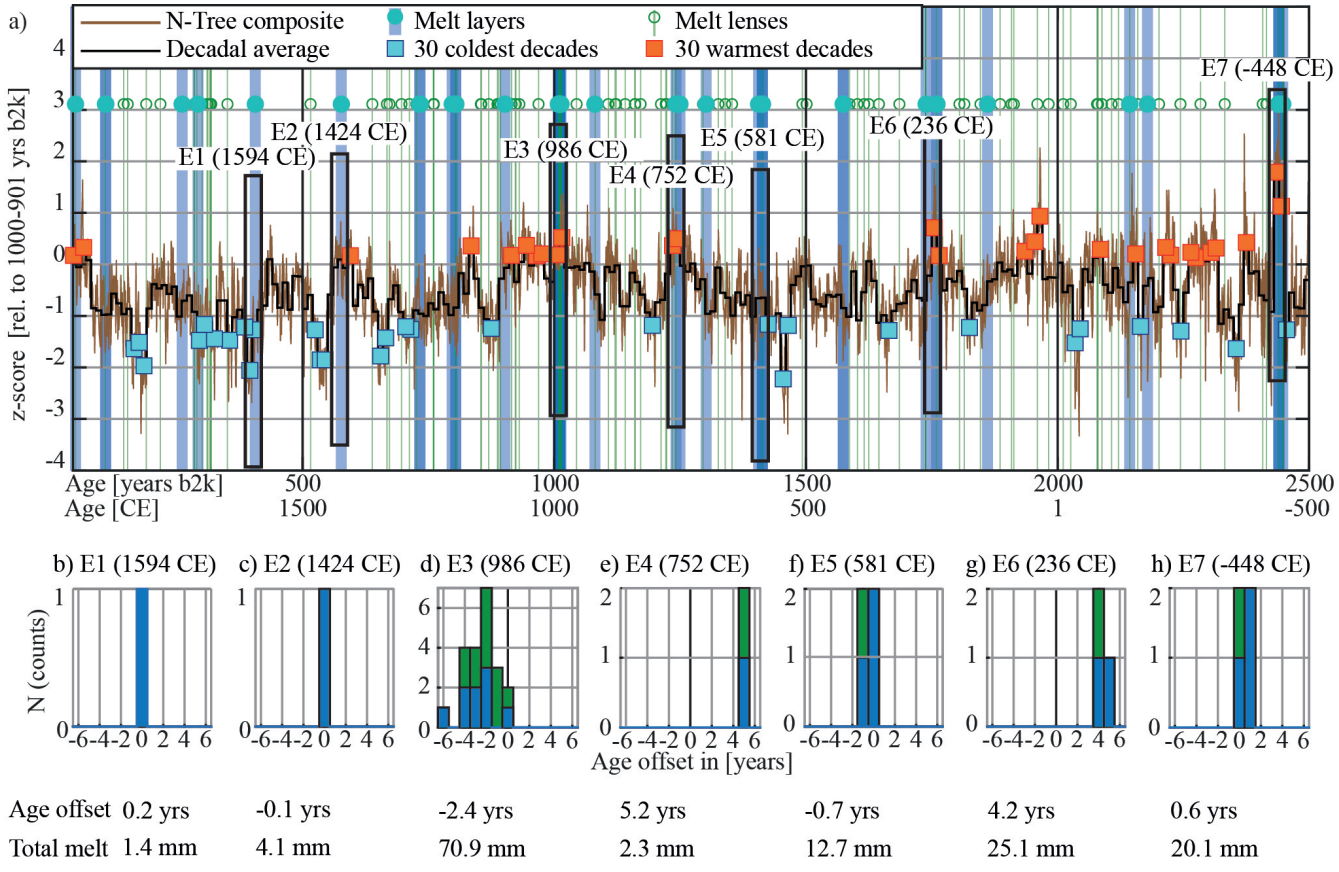

Figure 14. a) Tree-ring growth anomaly (brown, Sigl et al., 2015) compared to melt from 44 to 2500 years b2k. Melt layers (blue) and lenses (green) are highlighted at the corresponding age by vertical bars. Seven melt events (E1 to E7) are highlighted with black boxes. Decadal average (black line), 30 warmest and coldest decades as orange and light blue boxes, respectively. b -h) histograms of age offset form the melt events (layers in blue, lenses in green) to the largest tree-ring growth year, within ±6 years. The exceptional 986 CE event (E3) is younger than the tree-ring maximum by about 2.4 years.

proximity. For the 986 CE event (fig. 14d), a considerable melt event in our record, we find a tree ring warm year which is about 2.4 years older.

We analyze the 30 warmest and 30 coldest decades derived from tree ring data and find four to five times more melt events in decades with enhanced tree ring growth, compared to those with limited tree growth (tab. 1). This indicates a clear connection between warmer summers in the Northern Hemisphere derived from tree ring data and warmer summers over the central Greenland ice sheet.

Melting at EastGRIP might not be synchronous with all tree-ring peaks, but still offers some insight to the correlation of melt and tree ring growth on a larger geographic scale. This is also the case for volcanic eruptions: many volcanic events do not

https://doi.org/10.5194/cp-2021-89
Preprint. Discussion started: 16 July 2021

Climate of the Past Discussions

Table 1. Number of melt events in the 30 warmest, 30 coldest decades, and all decades (orange and blue boxes and black line, respectively, in fig. 14). The uncertainties are estimated only by considering the uncertain melt events. The size of z-scores can be considered a proxy for temperature. In periods with higher z-scores, meaning warmer periods with thicker tree rings, we find significantly more melt events. Periods with lower z-scores, i.e. colder decades, contain fewer melt events.

	30 warmest decades	30 coldest decades	all decades
Melt events per decade	1.48 ± 0.09	0.37 ± 0.10	0.59 ± 0.058
z-score from Temperate value	+8.3	-1.9	

correspond to deep cooling in the tree ring records, although local minima are often observed in correspondence (Sinnl et al, in prep.). Due to the age uncertainty of melt events and difficulties in time-scale translations, we cannot evaluate a more precise age-offset further. Moreover, even though more melting occurs during tree-ring warm-decades, not every prominent peak in the tree-ring record has melt events in its proximity.

The location of EastGRIP might not represent the complexity of the climatic dynamics that produces tree ring growth anomalies at scattered locations around the Northern Hemisphere, but the occurrence of more melt in warm periods and in proximity of some of the warmest years suggests a partial correlation. We expect that future studies could improve the results we have presented, in particular for the correlation of the melt events at EastGRIP with other ice cores and with more temperature records from around the globe.

4.7 The first Viking voyages to Greenland

In the summer of 986 CE the Viking Erik the Red sailed from Iceland to Greenland for the first time ever (Anderson, 1891; Brooks, 1986). This year coincides with the exceptional 986 CE melt event in Greenland, and could hint to why the Vikings chose this year for their voyage. A warm summer could mean less sea ice extent, and thus easier access to the Greenlandic coast and a safer voyage. Later in the same year, in an attempt to follow Erik the Red to Greenland, the Viking Bjarne Herjulfson got lost in thick fog and discovered America by accident (Brooks, 1986).

However, the literature disagrees, whether the Viking Erik the Red sailed to Greenland in 986 CE (Anderson, 1891; Brooks, 1986), if this happened in the year 985 CE (Jakobsen, 2017), or if he departed to Greenland in 983 CE and returned to Iceland in 986 CE (Fitzhugh, 2000). Just like the historical literature has uncertainties, so does our melt layer age. Uncertainties can be in the depth-age correlation of our ice core or because of melt percolating into the snow pack, thus disrupting the stratigraphy. In the tree ring record, a compilation claiming no uncertainties, the year 986 CE also stands out as an exceptionally warm summer across the Northern Hemisphere (Sigl et al., 2015).

While there is an uncertainty in the age of melt events in Greenland and also in the historical documentation of Viking voyages, these two events do align. We therefore suggest, that an exceptionally warm summer in the North Atlantic region could be a possible explanation of why the Vikings chose this year for their first voyage between Iceland and Greenland.

https://doi.org/10.5194/cp-2021-89
Preprint. Discussion started: 16 July 2021


Climate of the Past Discussions

5 Conclusion

Compared to other ice cores from Renland, coastal Greenland (Taranczewski et al., 2019) or northern Canada (Fisher et al., 2012), we do not find much melt in the EastGRIP ice core. In total only 831 mm over 10,000 years. Here we must keep in mind that the average summer temperature at EastGRIP lays around -25 °C, making melt events a rare phenomenon. It is therefore almost surprising that we find 137 melt layers and 424 melt lenses at a site with such cold summers.

We correct for thinning of layers due to vertical compression with depth, but including the upstream effects remains a challenge. It is possible that temperatures rise by 3 °C soley due to EastGRIP site flowing downstream with NEGIS, but the number of melt layers per 100 years does not increase in the expected rate (Alley and Anandakrishnan, 1995). With a gradual cooling throughout the Holocene (Axford et al., 2021), the temperature changes at EastGRIP are hard to quantify. Nevertheless, warm and cold periods throughout the Holocene stand out in our record.

Our figures of melt layer thickness (fig. 7), melt event frequency (fig. 9), melt events per 100 years (fig. 10), or melt per century (fig. 11) can all be seen as a climatic signal (as compiled in fig. 12). We clearly identify periods with very few to no melt events, i.e. cooler periods, and periods with an abundance of melt events, i.e. warmer periods. These match generally accepted climatic periods such as the Medieval and Roman warm periods, the HCO, or the 8.2 kyr cooling event.

When analyzing melt layers on an annual time scale, the well-studied 2012-melt event in Greenland (e.g. Nghiem et al., 2012; Bonne et al., 2015; Nilsson et al., 2015) helps our understanding of natural melt events. Melt, in general, does not remain on the surface but percolates into the snowpack, creating melt layers in greater depths disturbing the linear time relationship of the stratigraphy (fig. 2). When analyzing melt layers on an annual time scale, one must thus take into account this complicated surface melt water percolation, which is not reconstructable from the finished picture of melt layers in ice cores.

In hindsight it is not possible to distinguish between two scenarios: 1) five consecutive years with surface melting each summer, which then create a melt layer in each of the corresponding snow layers, or 2) one large melt and rain event, which creates melt layers scattered across all the snow from the last five years below. For smaller events the first options seems likely. For larger events, creating thick melt layers, the chances are high that melt percolates deep into the wet and warm snow pack, disrupting the stratigraphic order. Thus, when comparing melt layer data to other data, such as isotopes, impurities, weather stations, or tree rings, we introduce an unknown offset of a few years, which is different for each event. This parasitic infiltration of layers from different years into the stratigraphy, could potentially ruin the consistency of, e.g. isotope records assuming the stratigraphy to be linear in time. This certainly adds another factor of complication to the tempo-spatial variability recently observed and discussed (e.g. Münch and Laepple, 2018; Steen-Larsen et al., 2011).

When we compare this work to tree rings (Sigl et al., 2015), peaks in the melt layer and tree ring data align (with an offset of a few years, see above). The large melt events also stand out in the tree ring record and hint to outstanding warm summers being a phenomenon over the entire northern hemisphere. While this is not strictly in agreement with our understanding of atmospheric circulations (e.g. Bonne et al., 2015; Hanna et al., 2016; Graeter et al., 2018), the effect could also only be on some trees used in the tree ring composite, introducing a warm bias for these certain years.

https://doi.org/10.5194/cp-2021-89
Preprint. Discussion started: 16 July 2021


Climate of the Past Discussions

So far, the 986 CE and 2012 CE melt events are unprecedented in the Holocene. Both events historically stand out: the 986 CE warm event marks the beginning of Viking voyages to Greenland and the 2012 CE event is the only documented rain event in the central area of the Greenland ice sheet. Although the 2012-melt event is considered an exception it could be a hint to what we can expect for future summers in Greenland as global warming proceeds. The measured thickness of the 2012 melt layer is 3.5 cm (fig. 1c). Even after correcting for thinning, this makes it by a factor of two, by far the thickest melt layer we find in the last 10,000 years (compare to fig. 7). After gradual burial and metamorphism of snow layers, and thus thinning out the porous snow between the solid melt layers, the 2012 melt event will have a similar appearance in the stratigraphy as the 986 CE event (fig. 2d). These two events clearly stand out over the past 10,000 years, and it is not a coincidence that they are located in the most recent part of the Holocene.

https://doi.org/10.5194/cp-2021-89
Preprint. Discussion started: 16 July 2021

References

Alley, R. and Koci, B.: Ice-Core Analysis at Site A, Greenland: Preliminary Results, Annals of Glaciology, 10, 1–4, https://doi.org/10.3189/s0260305500004067, 1988.

Alley, R. B. and Anandakrishnan, S.: Variations in melt-layer frequency in the GISP2 ice core: implications for Holocene summer temperatures in central Greenland, Annals of Glaciology, 21, 64–70, https://doi.org/10.3189/s0260305500015615, 1995.

Alley, R. B., Gow, A. J., Meese, D. A., Fitzpatrick, J. J., and Waddington, E. D.: Grain-scale processes, folding, and stratigraphic, Journal of Geophysical Research, 102, 26 819–26 830, 1997.

Anderson, R. B.: America not discovered by Columbus : an historical sketch of the discovery of America by the Norsemen in the tenth century, Chicago: SC Griggs, 1891, 1 edn., 1891.

Axford, Y., de Vernal, A., and Osterberg, E. C.: Past Warmth and Its Impacts During the Holocene Thermal Maximum in Greenland, Annual Review of Earth and Planetary Sciences, 49, 279–307, https://doi.org/10.1146/annurev-earth-081420-063858, 2021.

Bennartz, R., Shupe, M. D., Turner, D. D., Walden, V. P., Steffen, K., Cox, C. J., Kulie, M. S., Miller, N. B., and Pettersen, C.: July 2012 Greenland melt extent enhanced by low-level liquid clouds, Nature, 496, 83–86, https://doi.org/10.1038/nature12002, 2013.

Berger, A. and Loutre, M. F.: Insolation values for the climate of the last 10 million years, Quaternary Science Reviews, 10, 297–317, https://doi.org/10.1016/0277-3791(91)90033-Q, 1991.

Boers, N. and Rypdal, M.: Critical slowing down suggests that the western Greenland Ice Sheet is close to a tipping point, Proceedings of the National Academy of Sciences of the United States of America, 118, 1–7, https://doi.org/10.1073/pnas.2024192118, 2021.

Bonne, J. L., Steen-Larsen, H. C., Risi, C., Werner, M., Sodemann, H., Lacour, J. L., Fettweis, X., Cesana, G., Delmotte, M., Cattani, O., Vallelonga, P., Kjær, H. A., Clerbaux, C., Sveinbjörnsdóttir, Á. E., and Masson-Delmotte, V.: The summer 2012 Greenland heat wave: In situ and remote sensing observations of water vapor isotopic composition during an atmospheric river event, Journal of Geophysical Research, 120, 2970–2989, https://doi.org/10.1002/2014JD022602, 2015.

Bova, S., Rosenthal, Y., Liu, Z., Godad, S. P., and Yan, M.: Seasonal origin of the thermal maxima at the Holocene and the last interglacial, Nature, 589, 548–553, https://doi.org/10.1038/s41586-020-03155-x, http://dx.doi.org/10.1038/s41586-020-03155-x, 2021.

Brooks, A. S.: Vinland Revisited: 986-1986, Smithsonian Institution Press Washington DC, 8, 1–5, 1986.

Brunt, D.: The adiabatic lapse-rate for dry and saturated air, Quarterly Journal of the Royal Meteorological Society, 59, 351–360, https://doi.org/https://doi.org/10.1002/qj.49705925204, 1933.

Buizert, C., Martinerie, P., Petrenko, V. V., Severinghaus, J. P., Trudinger, C. M., Witrant, E., Rosen, J. L., Orsi, A. J., Rubino, M., Etheridge, D. M., Steele, L. P., Hogan, C., Laube, J. C., Sturges, W. T., Levchenko, V. A., Smith, A. M., Levin, I., Conway, T. J., Dlugokencky, E. J., Lang, P. M., Kawamura, K., Jenk, T. M., White, J. W., Sowers, T., Schwander, J., and Blunier, T.: Gas transport in firn: Multiple-tracer characterisation and model intercomparison for NEEM, Northern Greenland, Atmospheric Chemistry and Physics, 12, 4259–4277, https://doi.org/10.5194/acp-12-4259-2012, 2012.

Buizert, C., Keisling, B. A., Box, J. E., He, F., Carlson, A. E., Sinclair, G., and DeConto, R. M.: Greenland-Wide Seasonal Temperatures During the Last Deglaciation, Geophysical Research Letters, 45, 1905–1914, https://doi.org/10.1002/2017GL075601, 2018.

Cohen, K. M., Finney, S. C., Gibbard, P. L., and Fan, J. X.: International Chronostratigraphic Chart, The ICS International Chronostratigraphic Chart, 36, 199–204, http://www.stratigraphy.org/ICSchart/ChronostratChart2016-04.pdf, 2016.

Dahl-Jensen, D., Mosegaard, K., Gundestrup, N., Clow, G. D., Johnsen, S. J., Hansen, A. W., and Balling, N.: Past temperatures directly from the Greenland Ice Sheet, Science, 282, 268–271, https://doi.org/10.1126/science.282.5387.268, 1998.

https://doi.org/10.5194/cp-2021-89
Preprint. Discussion started: 16 July 2021

Dalton, A. S., Margold, M., Stokes, C. R., Tarasov, L., Dyke, A. S., Adams, R. S., Allard, S., Arends, H. E., Atkinson, N., Attig, J. W., Barnett, P. J., Barnett, R. L., Batterson, M., Bernatchez, P., Borns, H. W., Breckenridge, A., Briner, J. P., Brouard, E., Campbell, J. E., Carlson, A. E., Clague, J. J., Curry, B. B., Daigneault, R. A., Dubé-Loubert, H., Easterbrook, D. J., Franzi, D. A., Friedrich, H. G., Funder, S., Gauthier, M. S., Gowan, A. S., Harris, K. L., Hétu, B., Hooyer, T. S., Jennings, C. E., Johnson, M. D., Kehew, A. E., Kelley, S. E., Kerr, D., King, E. L., Kjeldsen, K. K., Knaeble, A. R., Lajeunesse, P., Lakeman, T. R., Lamothe, M., Larson, P., Lavoie, M., Loope, H. M., Lowell, T. V., Lusardi, B. A., Manz, L., McMartin, I., Nixon, F. C., Occhietti, S., Parkhill, M. A., Piper, D. J., Pronk, A. G., Richard, P. J., Ridge, J. C., Ross, M., Roy, M., Seaman, A., Shaw, J., Stea, R. R., Teller, J. T., Thompson, W. B., Thorleifson, L. H., Utting, D. J., Veillette, J. J., Ward, B. C., Weddle, T. K., and Wright, H. E.: An updated radiocarbon-based ice margin chronology for the last deglaciation of the North American Ice Sheet Complex, Quaternary Science Reviews, 234, https://doi.org/10.1016/j.quascirev.2020.106223, 2020.

Das, S. B. and Alley, R. B.: Characterization and formation of melt layers in polar snow : observations and experiments from West Antarctica, Journal of Glaciology, 51, 307–312, 2005.

Dash, J. G., Rempel, A. W., and Wettlaufer, J. S.: The physics of premelted ice and its geophysical consequences, Reviews of Modern Physics, 78, 695–741, https://doi.org/10.1103/RevModPhys.78.695, 2006.

Faria, S. H., Kipfstuhl, S., and Lambrecht, A.: The EPICA-DML Deep Ice Core, Springer-Verlag GmbH Germany, Berlin, 2018.

Fegyveresi, J. M., Alley, R. B., Muto, A., Orsi, A. J., and Spencer, M. K.: Surface formation, preservation, and history of low-porosity crusts at the WAIS Divide site, West Antarctica, Cryosphere, 12, 325–341, https://doi.org/10.5194/tc-12-325-2018, 2018.

Fisher, D., Zheng, J., Burgess, D., Zdanowicz, C., Kinnard, C., Sharp, M., and Bourgeois, J.: Recent melt rates of Canadian arctic ice caps are the highest in four millennia, Global and Planetary Change, 84-85, 3–7, https://doi.org/10.1016/j.gloplacha.2011.06.005, http://dx.doi.org/10.1016/j.gloplacha.2011.06.005, 2012.

Fisher, D. A., Koerner, R. M., and Reeh, N.: Holocene climatic records from Agassiz Ice Cap, Ellesmere Island, NWT, Canada, Holocene, 5, 19–24, https://doi.org/10.1177/095968369500500103, 1995.

Fitzhugh, W. W.: Puffins, ringed pins, and runestones: the Viking passage to America, Smithsonian Institution Press Washington DC, pp. 11–25, 2000.

Fritzsche, D., Schütt, R., Meyer, H., Miller, H., Wilhelms, F., Opel, T., and Savatyugin, L. M.: A 275 year ice-core record from Akademii Nauk ice cap, Severnaya Zemlya, Russian Arctic, Annals of Glaciology, 42, 361–366, https://doi.org/10.3189/172756405781812862, 2005.

Gardner, A. S., Sharp, M. J., Koerner, R. M., Labine, C., Boon, S., Marshall, S. J., Burgess, D. O., and Lewis, D.: Near-surface temperature lapse rates over arctic glaciers and their implications for temperature downscaling, Journal of Climate, 22, 4281–4298, https://doi.org/10.1175/2009JCLI2845.1, 2009.

Gerber, T. A., Hvidberg, C. S., Rasmussen, S. O., Franke, S., Sinnl, G., Grinsted, A., Jansen, D., and Dahl-jensen, D.: Upstream flow effects revealed in the EastGRIP ice core using a Monte Carlo inversion of a two-dimensional ice-flow model, The Cryosphere, 2021.

Graeter, K. A., Osterberg, E. C., Ferris, D. G., Hawley, R. L., Marshall, H. P., Lewis, G., Meehan, T., McCarthy, F., Overly, T., and Birkel, S. D.: Ice Core Records of West Greenland Melt and Climate Forcing, Geophysical Research Letters, 45, 3164–3172, https://doi.org/10.1002/2017GL076641, 2018.

Hanna, E., Cropper, T. E., Hall, R. J., and Cappelen, J.: Greenland Blocking Index 1851–2015: a regional climate change signal, International Journal of Climatology, 36, 4847–4861, https://doi.org/10.1002/joc.4673, 2016.

Herron, M. M., Herron, S. L., and Langway, C. C.: Climatic signal of ice melt features in southern Greenland, Nature, 293, 389–391, https://doi.org/10.1038/293389a0, 1981.

https://doi.org/10.5194/cp-2021-89
Preprint. Discussion started: 16 July 2021

Humphrey, N. F., Harper, J. T., and Pfeffer, W. T.: Thermal tracking of meltwater retention in Greenland ' s accumulation area, Journal of Geophysical Research, 117, 1–11, https://doi.org/10.1029/2011JF002083, 2012.

Hvidberg, C. S., Grinsted, A., Dahl-Jensen, D., Khan, S. A., Kusk, A., Andersen, J. K., Neckel, N., Solgaard, A., Karlsson, N. B., Kjar, H. A., and Vallelonga, P.: Surface velocity of the Northeast Greenland Ice Stream (NEGIS): Assessment of interior velocities derived from satellite data by GPS, Cryosphere, 14, 3487–3502, https://doi.org/10.5194/tc-14-3487-2020, 2020.

Jakobsen, S.-M. E.: Turen går til Vikingtiden, vol. 1, JP/Politikens Hus A/S, København, 2017.

Jansen, D., Llorens, M. G., Westhoff, J., Steinbach, F., Kipfstuhl, S., Bons, P. D., Griera, A., and Weikusat, I.: Small-scale disturbances in the stratigraphy of the NEEM ice core: Observations and numerical model simulations, The Cryosphere, 10, 359–370, https://doi.org/10.5194/tc-10-359-2016, 2016.

Kameda, T., Narita, H., Shoji, H., Nishio, F., Fujii, Y., and Watanabe, O.: Melt features in ice cores from site J, souther Greenland: some implications for summer cliamte since AD 1550, Annals of Glaciology, pp. 51–58, 1995.

Keegan, K. M., Albert, M. R., McConnell, J. R., and Baker, I.: Climate change and forest fires synergistically drive widespread melt events of the Greenland Ice Sheet, Proceedings of the National Academy of Sciences of the United States of America, 111, 7964–7967, https://doi.org/10.1073/pnas.1405397111, 2014.

Kipfstuhl, S., Pauer, F., Kuhs, W. F., and Shoji, H.: Air bubbles and clathrate hydrates in the transition zone ofthe NGRIP deep ice core, Geophysical Research Letters, 28, 591–594, https://doi.org/10.1029/1999GL006094, 2001.

Koerner, R. M. and Fisher, D. A.: A record of Holocene summer climate from a Canadian high-Arctic ice core, Nature, 343, 630–631, https://doi.org/10.1038/343630a0, 1990.

Langway, C. C. and Shoji, H.: Past temperature record from the analysis of melt features in the DYE3, Grennland, ice core, Annals of Glaciology, 14, 343–344, 1990.

Lecavalier, B. S., Milne, G. A., Vinther, B. M., Fisher, D. A., Dyke, A. S., and Simpson, M. J.: Revised estimates of Greenland ice sheet thinning histories based on ice-core records, Quaternary Science Reviews, 63, 73–82, https://doi.org/10.1016/j.quascirev.2012.11.030, http://dx.doi.org/10.1016/j.quascirev.2012.11.030, 2013.

Llorens, M. G., Griera, A., Steinbach, F., Bons, P. D., Gomez-Rivas, E., Jansen, D., Roessiger, J., Lebensohn, R. A., and Weikusat, I.: Dynamic recrystallization during deformation of polycrystalline ice: Insights from numerical simulations, Philosophical Transactions of the Royal Society A: Mathematical, Physical and Engineering Sciences, 375, https://doi.org/10.1098/rsta.2015.0346, 2017.

McGwire, K. C., Hargreaves, G. M., Alley, R. B., Popp, T. J., Reusch, D. B., Spencer, M. K., and Taylor, K. C.: An integrated system for optical imaging of ice cores, Cold Regions Science and Technology, 53, 216–228, https://doi.org/10.1016/j.coldregions.2007.08.007, 2008.

Mojtabavi, S., Wilhelms, F., Cook, E., Davies, S., Sinnl, G., Skov Jensen, M., Dahl-Jensen, D., Svensson, A., Vinther, B., Kipfstuhl, S., Jones, G., Karlsson, N., Faria, S. H., Gkinis, V., Kjær, H., Erhardt, T., Berben, S., Nisancioglu, K., Koldtoft, I., and Rasmussen, S. O.: A first chronology for the East GReenland Ice-core Project (EGRIP) over the Holocene and last glacial termination, Climate of the Past Discussions, pp. 1–22, https://doi.org/10.5194/cp-2019-143, 2020.

Monnin, E., Steig, E. J., Siegenthaler, U., Kawamura, K., Schwander, J., Stauffer, B., Stocker, T. F., Morse, D. L., Barnola, J. M., Bellier, B., Raynaud, D., and Fischer, H.: Evidence for substantial accumulation rate variability in Antarctica during the Holocene, through synchronization of CO2 in the Taylor Dome, Dome C and DML ice cores, Earth and Planetary Science Letters, 224, 45–54, https://doi.org/10.1016/j.epsl.2004.05.007, 2004.

https://doi.org/10.5194/cp-2021-89
Preprint. Discussion started: 16 July 2021

Morcillo, G., Faria, S. H., and Kipfstuhl, S.: Unravelling Antarctica's past through the stratigraphy of a deep ice core: an image-analysis study of the EPICA-DML line-scan images, Quaternary International, https://doi.org/10.1016/j.quaint.2020.07.011, 2020.

Mote, T. L.: Greenland surface melt trends 1973-2007: Evidence of a large increase in 2007, Geophysical Research Letters, 34, 1–5, https://doi.org/10.1029/2007GL031976, 2007.

Münch, T. and Laepple, T.: What climate signal is contained in decadal - To centennial-scale isotope variations from Antarctic ice cores?, Climate of the Past, 14, 2053–2070, https://doi.org/10.5194/cp-14-2053-2018, 2018.

Neff, P. D.: A review of the brittle ice zone in polar ice cores, Annals of Glaciology, 55, 72–82, https://doi.org/10.3189/2014AoG68A023, 2014.

Nghiem, S. V., Hall, D. K., Mote, T. L., Tedesco, M., Albert, M. R., Keegan, K., Shuman, C. A., DiGirolamo, N. E., and Neumann, G.: The extreme melt across the Greenland ice sheet in 2012, Geophysical Research Letters, 39, 6–11, https://doi.org/10.1029/2012GL053611, 2012.

Nilsson, J., Vallelonga, P., Simonsen, S. B., Sørensen, L. S., Forsberg, R., Dahl-Jensen, D., Hirabayashi, M., Goto-Azuma, K., Hvidberg, C. S., Kjær, H. A., and Satow, K.: Greenland 2012 melt event effects on CryoSat-2 radar altimetry, Geophysical Research Letters, 42, 3919–3926, https://doi.org/10.1002/2015GL063296, 2015.

NorthGRIPmembers: High-resolution record of Northern Hemisphere climate extending into the last interglacial period, Nature, 431, 147–151, 2004.

Ohmura, A.: Physical basis for the temperature-based melt-index method, Journal of Applied Meteorology, 40, 753–761, https://doi.org/10.1175/1520-0450(2001)040<0753:PBFTTB>2.0.CO;2, 2001.

Orsi, A. J., Kawamura, K., Fegyveresi, J. M., Headly, M. A., Alley, R. B., and Severinghaus, J. P.: Differentiating bubble-free layers from Melt layers in ice cores using noble gases, Journal of Glaciology, 61, 585–594, https://doi.org/10.3189/2015JoG14J237, 2015.

Pfeffer, W. T. and Humphrey, N. F.: Fortmation of ice layers by infiltration and refreezing of meltwater, Annals of Glaciology, 26, 83–91, 1998.

Rasmussen, S. O., Andersen, K. K., Svensson, A. M., Steffensen, J. P., Vinther, B. M., Clausen, H. B., Siggaard-Andersen, M. L., Johnsen, S. J., Larsen, L. B., Dahl-Jensen, D., Bigler, M., Röthlisberger, R., Fischer, H., Goto-Azuma, K., Hansson, M. E., and Ruth, U.: A new Greenland ice core chronology for the last glacial termination, Journal of Geophysical Research Atmospheres, 111, 1–16, https://doi.org/10.1029/2005JD006079, 2006.

Rasmussen, S. O., Vinther, B. M., Clausen, H. B., and Andersen, K. K.: Early Holocene climate oscillations recorded in three Greenland ice cores, Quaternary Science Reviews, 26, 1907–1914, https://doi.org/10.1016/j.quascirev.2007.06.015, 2007.

Schaller, C. F.: Towards understanding the signal formation in polar snow, firn and ice using X-ray computed tomography, PhD Thesis, p. 68, https://doi.org/10.1088/1751-8113/44/8/085201, 2018.

Schaller, C. F., Freitag, J., Kipfstuhl, S., Laepple, T., Christian Steen-Larsen, H., and Eisen, O.: A representative density profile of the North Greenland snowpack, Cryosphere, 10, 1991–2002, https://doi.org/10.5194/tc-10-1991-2016, 2016.

Shoji, H. and Langway, C.: HYDRATE-BUBBLE . TRANSFORMATION PROCESS IN GLACIER ICE, Journal de Physique, 3, 551–556, 1987.

Sigl, M., Winstrup, M., McConnell, J. R., Welten, K. C., Plunkett, G., Ludlow, F., Büntgen, U., Caffee, M., Chellman, N., Dahl-Jensen, D., Fischer, H., Kipfstuhl, S., Kostick, C., Maselli, O. J., Mekhaldi, F., Mulvaney, R., Muscheler, R., Pasteris, D. R., Pilcher, J. R., Salzer, M., Schüpbach, S., Steffensen, J. P., Vinther, B. M., and Woodruff, T. E.: Timing and climate forcing of volcanic eruptions for the past 2,500 years, Nature, 523, 543–549, https://doi.org/10.1038/nature14565, 2015.

https://doi.org/10.5194/cp-2021-89
Preprint. Discussion started: 16 July 2021

Simonsen, M. F., Baccolo, G., Blunier, T., Borunda, A., Delmonte, B., Frei, R., Goldstein, S., Grinsted, A., Kjær, H. A., Sowers, T., Svensson, A., Vinther, B., Vladimirova, D., Winckler, G., Winstrup, M., and Vallelonga, P.: East Greenland ice core dust record reveals timing of Greenland ice sheet advance and retreat, Nature Communications, 10, https://doi.org/10.1038/s41467-019-12546-2, http://dx.doi.org/10.1038/s41467-019-12546-2, 2019.

Steen-Larsen, H. C., Masson-Delmotte, V., Sjolte, J., Johnsen, S. J., Vinther, B. M., Bréon, F. M., Clausen, H. B., Dahl-Jensen, D., Falourd, S., Fettweis, X., Gallée, H., Jouzel, J., Kageyama, M., Lerche, H., Minster, B., Picard, G., Punge, H. J., Risi, C., Salas, D., Schwander, J., Steffen, K., Sveinbjörnsdóttir, A. E., Svensson, A., and White, J.: Understanding the climatic signal in the water stable isotope records from the NEEM shallow firn/ice cores in northwest Greenland, Journal of Geophysical Research Atmospheres, 116, 1–20, https://doi.org/10.1029/2010JD014311, 2011.

Steinbach, F., Bons, P. D., Griera, A., Jansen, D., Llorens, M. G., Roessiger, J., and Weikusat, I.: Strain localization and dynamic recrystallization in the ice-air aggregate: A numerical study, Cryosphere, 10, 3071–3089, https://doi.org/10.5194/tc-10-3071-2016, 2016.

Svensson, A., Nielsen, S. W., Kipfstuhl, S., Johnsen, S. J., Steffensen, J. P., Bigler, M., Ruth, U., and Röthlisberger, R.: Visual stratigraphy of the North Greenland Ice Core Project (NorthGRIP) ice core during the last glacial period, Journal of Geophysical Research: Atmospheres, 110, 1–11, https://doi.org/10.1029/2004JD005134, 2005.

Taranczewski, T., Freitag, J., Eisen, O., Vinther, B., Wahl, S., and Kipfstuhl, S.: 10,000 years of melt history of the 2015 Renland ice core, EastGreenland, The Cryosphere Discussions, pp. 1–16, https://doi.org/10.5194/tc-2018-280, 2019.

Tedesco, M., Fettweis, X., Mote, T., Wahr, J., Alexander, P., Box, J. E., and Wouters, B.: Evidence and analysis of 2012 Greenland records from spaceborne observations, a regional climate model and reanalysis data, The Cryosphere, 7, 615–630, https://doi.org/10.5194/tc-7-615-2013, 2013.

Thomas, E. R., Wolff, E. W., Mulvaney, R., Steffensen, J. P., Johnsen, S. J., Arrowsmith, C., White, J. W., Vaughn, B., and Popp, T.: The 8.2 ka event from Greenland ice cores, Quaternary Science Reviews, 26, 70–81, https://doi.org/10.1016/j.quascirev.2006.07.017, 2007.

Trusel, L. D., Das, S. B., Osman, M. B., Evans, M. J., Smith, B. E., Fettweis, X., McConnell, J. R., Noël, B. P., and van den Broeke, M. R.: Nonlinear rise in Greenland runoff in response to post-industrial Arctic warming, Nature, 564, 104–108, https://doi.org/10.1038/s41586-018-0752-4, http://dx.doi.org/10.1038/s41586-018-0752-4, 2018.

Uchida, T., Yasuda, K., Oto, Y., Shen, R., and Ohmura, R.: Natural supersaturation conditions needed for nucleation of air-clathrate hydrates in deep ice sheets, Journal of Glaciology, 60, 1135–1139, https://doi.org/10.3189/2014JoG13J232, 2014.

Vallelonga, P., Christianson, K., Alley, R. B., Anandakrishnan, S., Christian, J. E., Dahl-Jensen, D., Gkinis, V., Holme, C., Jacobel, R. W., Karlsson, N. B., Keisling, B. A., Kipfstuhl, S., Kjær, H. A., Kristensen, M. E., Muto, A., Peters, L. E., Popp, T., Riverman, K. L., Svensson, A. M., Tibuleac, C., Vinther, B. M., Weng, Y., and Winstrup, M.: Initial results from geophysical surveys and shallow coring of the Northeast Greenland Ice Stream (NEGIS), Cryosphere, 8, 1275–1287, https://doi.org/10.5194/tc-8-1275-2014, 2014.

Vinther, B. M., Clausen, H. B., Johnsen, S. J., Rasmussen, S. O., Andersen, K. K., Buchardt, S. L., Dahl-Jensen, D., Seierstad, I. K., Siggaard-Andersen, M. L., Steffensen, J. P., Svensson, A., Olsen, J., and Heinemeier, J.: A synchronized dating of three Greenland ice cores throughout the Holocene, Journal of Geophysical Research Atmospheres, 111, 1–11, https://doi.org/10.1029/2005JD006921, 2006.

Vinther, B. M., Buchardt, S. L., Clausen, H. B., Dahl-Jensen, D., Johnsen, S. J., Fisher, D. A., Koerner, R. M., Raynaud, D., Lipenkov, V., Andersen, K. K., Blunier, T., Rasmussen, S. O., Steffensen, J. P., and Svensson, A. M.: Holocene thinning of the Greenland ice sheet, Nature, 461, 385–388, https://doi.org/10.1038/nature08355, http://dx.doi.org/10.1038/nature08355, 2009.

Waddington, E. D., Bolzan, J. F., and Alley, R. B.: Potential for stratigraphic folding near ice-sheet centers, Journal of Glaciology, 47, 639–648, https://doi.org/10.3189/172756501781831756, 2001.

https://doi.org/10.5194/cp-2021-89
Preprint. Discussion started: 16 July 2021

Weikusat, C., Kipfstuhl, S., and Weikusat, I.: Raman tomography of natural air hydrates, Journal of Glaciology, 61, 923–930, https://doi.org/10.3189/2015JoG15J009, 2015.

Weinhart, A. H., Kipfstuhl, S., Hörhold, M., Eisen, O., and Freitag, J.: Spatial Distribution of Crusts in Antarctic and Greenland Snowpacks and Implications for Snow and Firn Studies, Frontiers in Earth Science, 9, 1–16, https://doi.org/10.3389/feart.2021.630070, 2021.

Westhoff, J., Stoll, N., Franke, S., Weikusat, I., Bons, P., Kerch, J., Jansen, D., Kipfstuhl, S., and Dahl-Jensen, D.: A Stratigraphy Based Method for Reconstructing Ice Core Orientation, Annals of Glaciology, pp. 1–12, https://doi.org/doi.org/10.1017/aog.2020.76, 2020.

Winski, D., Osterberg, E., Kreutz, K., Wake, C., Ferris, D., Campbell, S., Baum, M., Bailey, A., Birkel, S., Introne, D., and Handley, M.: A 400-Year Ice Core Melt Layer Record of Summertime Warming in the Alaska Range, Journal of Geophysical Research: Atmospheres, 123, 3594–3611, https://doi.org/10.1002/2017JD027539, 2018.

Author contributions. Initial idea of manuscript and data acquisition by JW. Support on melt layers in ice cores in general came from AS, JF, SK, and DDJ. Coffee experiment and melt layer definition by SK. Tree ring to melt comparison by GS, idea by AS. Viking voyages and melt events by AS and JW. NEEM snowpit data and text by HAK and PV. Climatic interpretations and ice sheet evolution by BMV, AS, and JW. Comments on physical properties of melt layers and their appearance by IW and SK. JW prepared the manuscript with contributions and revisions from all co-authors.

Competing interests. The authors declare that they have no conflict of interest.

Acknowledgements. EastGRIP is directed and organized by the Centre for Ice and Climate at the Niels Bohr Institute, University of Copenhagen. It is supported by funding agencies and institutions in Denmark (A. P. Møller Foundation, University of Copenhagen), USA (US National Science Foundation, Office of Polar Programs), Germany (Alfred Wegener Institute, Helmholtz Centre for Polar and Marine Research), Japan (National Institute of Polar Research and Arctic Challenge for Sustainability), Norway (University of Bergen and Bergen Research Foundation), Switzerland (Swiss National Science Foundation), France (French Polar Institute Paul-Emile Victor, Institute for Geosciences and Environmental research) and China (Chinese Academy of Sciences and Beijing Normal University). JW, AS, BMV, SK, and DDJ thank the Villum Foundation, as this work was supported by the Villum Investigator Project IceFlow (NR. 16572). GS acknowledges support via the ChronoClimate project funded by the Carlsberg Foundation. IW acknowledges HGF funding (VH-NG-802).

Data availability. Once published, the data can be downloaded on the Centre for Ice and Climate home page: www.iceandclimate.nbi.ku.dk.